The transcriptional response to oxidative stress is independent of stress-granule formation

Amanjot Singh[a,*], Arvind Reddy Kandi[b,†], Deepa Jayaprakashappa[a,†], Guillaume Thuery[c], Devam J. Purohit[a], Joern Huelsmeier[c], Rashi Singh[a], Sai Shruti Pothapragada[a], Mani Ramaswami[a,c,*], and Baskar Bakthavachalu[b,d,*]

[a]National Centre for Biological Sciences, TIFR, Bangalore 560065, India; [b]Tata Institute for Genetics and Society Centre at inStem, Bellary Road, Bangalore 560065, India; [c]Trinity College Institute of Neuroscience, School of Genetics and Microbiology, Smurfit Institute of Genetics and School of Natural Sciences, Trinity College Dublin, Dublin-2, Ireland; [d]School of Basic Sciences, Indian Institute of Technology, Mandi 175005, India

ABSTRACT **Cells respond to stress with translational arrest, robust transcriptional changes, and transcription-independent formation of mRNP assemblies termed stress granules (SGs). Despite considerable interest in the role of SGs in oxidative, unfolded protein and viral stress responses, whether and how SGs contribute to stress-induced transcription have not been rigorously examined. To address this, we characterized transcriptional changes in *Drosophila* S2 cells induced by acute oxidative-stress and assessed how these were altered under conditions that disrupted SG assembly. Oxidative stress for 3 h predominantly resulted in induction or up-regulation of stress-responsive mRNAs whose levels peaked during recovery after stress cessation. The stress transcriptome is enriched in mRNAs coding for chaperones including HSP70s, small heat shock proteins, glutathione transferases, and several noncoding RNAs. Oxidative stress also induced cytoplasmic SGs that disassembled 3 h after stress cessation. As expected, RNAi-mediated knockdown of the conserved G3BP1/Rasputin protein inhibited SG assembly. However, this disruption had no significant effect on the stress-induced transcriptional response or stress-induced translational arrest. Thus SG assembly and stress-induced gene expression alterations appear to be driven by distinctive signaling processes. We suggest that while SG assembly represents a fast, transient mechanism, the transcriptional response enables a slower, longer-lasting mechanism for adaptation to and recovery from cell stress.**

Monitoring Editor
Karsten Weis
ETH Zurich

Received: Aug 25, 2021
Revised: Dec 14, 2021
Accepted: Dec 23, 2021

INTRODUCTION

Oxidative stress can have several cellular consequences, including DNA damage and increased levels of oxidized and misfolded proteins (Schieber and Chandel, 2014). It also activates components of the cellular integrated stress response (ISR) pathway, including stress kinases that modify the mRNA translational machinery (Gidalevitz *et al.*, 2011; Balchin *et al.*, 2016; Costa-Mattioli and Walter, 2020). Phosphorylation of the eukaryotic initiation factor, eIF2α, results in translational inhibition together with the formation of stress granules (SGs); cytoplasmic, liquid-liquid phase separated assemblies of translationally arrested mRNAs; RNA-binding proteins; and accessory components (which includes the preinitiation complex containing translation initiation factors and ribosomal proteins of the 40S ribosome subunit) (Kedersha *et al.*, 1999; Kedersha and Anderson, 2002; Ron, 2002; Wolozin and Ivanov, 2019). The formation of SGs has been well studied in response to different stresses and has been historically characterized by the presence of T-cell intracellular antigen-1 (TIA-1), polyA binding protein, and polyA RNA (Anderson and Kedersha, 2006; Anderson *et al.*, 2015).

Pathways and proteins involved in the ISR have been implicated in normal aging and in neurodegenerative disease (Radford *et al.*, 2015; Halliday *et al.*, 2017; Krukowski *et al.*, 2020). Increased levels

This article was published online ahead of print in MBoC in Press (http://www.molbiolcell.org/cgi/doi/10.1091/mbc.E21-08-0418) on January 5, 2022.

†Equal contribution.

*Address correspondence to: Mani Ramaswami (mani.ramaswami@tcd.ie); Baskar Bakthavachalu (baskar@iitmandi.ac.in); Amanjot Singh (amanjsingh@ncbs.res.in).

Abbreviations used: Atx2, Ataxin-2; 5-EU, 5-ethyl uridine; HSP, heat-shock protein; ISR, integrated stress response; ncRNA, noncoding RNA; rRNA, ribosomal RNA; SG, stress granule; snRNA, small nuclear RNA; snoRNA, small nucleolar RNA; TIA-1, T-cell intracellular antigen-1.

of oxidative stress are also thought to be associated with normal brain aging (Milton and Sweeney, 2012). Consistent with this, unusual SG-related neuronal inclusions have been observed in postmortem brain samples of aged but not young brains (Ginsberg *et al.*, 1998; Geser *et al.*, 2010; Bäuerlein *et al.*, 2017). SGs have gained even more significance since the discovery that protein inclusions associated with neurodegenerative diseases can contain SG components. In some cases, both inclusion formation and disease progression depend on factors that drive normal SG assembly (Gasset-Rosa *et al.*, 2019; Advani and Ivanov, 2020).

In addition to SG formation, oxidative stresses regulate transcription factors such as FOXO, HSF1, and Nrf2 to induce changes in the cellular transcriptome (Fedoroff, 2006; Donovan and Marr, 2015; Vihervaara *et al.*, 2018; Doonan *et al.*, 2019). In particular, stress increases the expression of mRNAs coding for cytoprotective proteins, including protein chaperones and modulators of lipid oxidation (Jacobson *et al.*, 2012). The third effect of acute oxidative stress is to induce translational arrest for the majority of cellular mRNAs. Here we ask whether these different stress responses occur independently of each other. In particular, we test whether signaling mediated through assembled SGs contributes to the transcriptional responses to oxidative stress as has been suggested by the role of SGs in signaling required for transcription of genes involved in viral defense (Fung *et al.*, 2013; Tsai and Lloyd, 2014; McCormick and Khaperskyy, 2017). It is intriguing as to how these two concurrent events are related as in some cases, protein aggregates require neither stress nor stress-associated transcription for assembly (Gasset-Rosa *et al.*, 2019). In cultured *Drosophila* S2 cells, we i) document the requirements and kinetics of SG formation and disassembly, ii) obtain robust data sets for stress-induced transcriptional changes during and after acute stress, and iii) examine how the stress-induced transcriptome and global mRNA translation is altered when SG assembly is perturbed. We address these issues in *Drosophila* cells partly for the ease with which SG assembly can be visualized and perturbed in these cells but mainly because *Drosophila* allows facile, future follow-up experiments to assess the function of stress-regulated genes in vivo.

As anticipated, *Drosophila* S2 cells acutely exposed to the well-known stressor sodium arsenite show robust formation of Ataxin-2 (Atx2), Rox8/TIA-1, and Rasputin (Rin)/Ras GTPase-activating protein-binding protein 1 (G3BP1) positive SGs along with simultaneous inhibition of global translation (Kedersha and Anderson, 2007; Jain *et al.*, 2016; Kedersha *et al.*, 2016; Wheeler *et al.*, 2016; Ivanov *et al.*, 2019; Escalante and Gasch, 2021). Parallel RNA-seq analyses show that arsenite stress also induces up-regulation of around 300 different transcripts. Following 3 h of poststress recovery in the absence of arsenite, SGs disassemble and become invisible. In contrast, the vast majority of stress-induced mRNAs remain up-regulated, consistent with a model in which SGs represent an acute protective mechanism that provides cells time to launch a longer-lasting transcription-dependent program for recovery from stress. In cells lacking Rin, although SGs are not visible, stress-induced translational arrest and stress-induced transcription remain unchanged. These data indicate SG formation is largely dispensable for oxidative-stress-induced changes to gene regulation.

RESULTS

Kinetics of assembly of arsenite-induced SGs in *Drosophila* S2 cells

To understand cellular changes occurring during oxidative stress and subsequent recovery, we employed sodium arsenite as a stressor in *Drosophila* S2 cells, an established cellular model for studying the stress response (Farny *et al.*, 2009; Aguilera-Gomez *et al.*, 2017). Consistent with prior observations (Farny *et al.*, 2009; Bakthavachalu *et al.*, 2018), we found that exposure of cells to 0.5 mM arsenite for 1 h leads to the formation of numerous Atx2 and Rin/G3BP positive SGs; these appeared larger and more distinct after 3 h of stress (Figure 1, Ai and ii, B, and C; Supplemental Figure S1A). To determine the temporal dynamics of clearance of SGs, we stressed the cells for 3 h, allowed them to recover by replacing the stressor with a fresh culture medium, and monitored SGs at specified time points afterward. The kinetics of granule formation and disassembly were quantified (Figure 1B). SGs are dynamic in nature and we capture snapshots of the granules at any particular time point (Jain *et al.*, 2016; Wheeler *et al.*, 2016); thus there can be cell-to-cell variation in the granule numbers. We find some cells still had granules but recovery from stress, in general, was accompanied by the progressive disappearance of SGs with a majority of cells having no or a few granules (Figure 1B; Supplemental Figure S1A). While some Atx2-positive granules remained after 1 h of recovery (Figure 1Aiv), none were visible after 3 h in most cells (Figure 1Av).

To address whether the disappearance of SGs after recovery correlated with reduced stress signaling, we assessed phosphorylation levels of eIF2α at S51 (Figure 1D). It is well established that stress kinases such as PEK and GCN2 phosphorylate eIF2α trigger arsenite-induced SG formation (Farny *et al.*, 2009). Consistent with this, we observed that eIF2α phosphorylation in S2 cells is elevated following either 1 or 3 h of exposure to arsenite (Figure 1D). After 3 h of arsenite removal, levels of eIF2α phosphorylation came down and were comparable to those under control conditions; importantly, there was no change in the expression of total eIF2α under any of these conditions (Figure 1D). Taken together, these observations confirm and extend previous findings in S2 cells (Farny *et al.*, 2009), showing that oxidative-stress induced SGs are transient, dynamic structures whose assembly/disassembly is concomitant with eIF2α phosphorylation that has been associated with the shutdown of cap-dependent protein translation (Hinnebusch, 2017; Adomavicius *et al.*, 2019).

Distinctive acute stress and post-stress ("recovery") transcriptomes

Genes transcriptionally regulated by stress could potentially encode factors involved in regulating the assembly and clearance of SGs or managing molecular or physiological consequences of stress. To identify molecules potentially involved in these processes, we examined transcriptional changes in S2 cells under acute stress conditions and following recovery when there are no visually detectable SGs. We isolated total RNA from cells that were i) untreated, ii) stressed for 3 h, and iii) recovered for 3 h following 3 h of stress and used RNA-Seq to identify and analyze polyA-selected RNA populations in each condition (Figure 2A). Three independent biological replicates were used for each of the three conditions. A total of more than 114 million high-quality reads (average ~10 million reads per sample) were generated and mapped to the *Drosophila* genome using STAR v2.5.3 (Supplemental File 2). The uniquely mapped reads for each sample were processed using HT-Seq and DESeq2 was used for normalization of transcript counts and differential expression. The correlation coefficient values demonstrate high similarity (0.992–1.0) across the biological replicates and clear differences in global transcriptomes during normal, stress, and recovery conditions (Figure 2B; Supplemental Figure S2A). Thus the analyses show that control transcriptomes differ significantly from those of cells during stress and following 3 h of recovery.

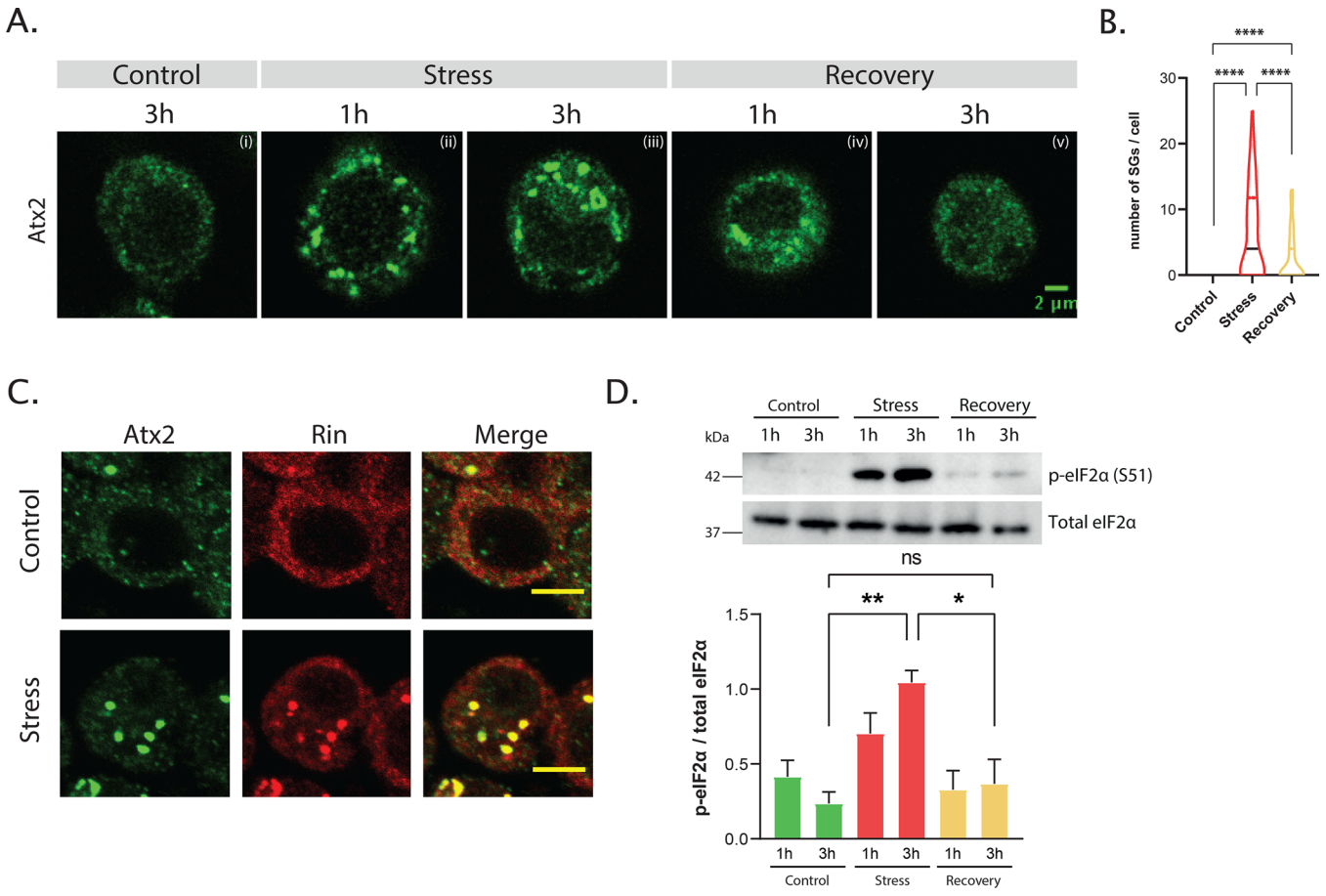

FIGURE 1: Kinetics of assembly of arsenite-induced SGs in *Drosophila* S2 cells. (A) Progression of arsenite-induced SGs assembly. Untreated S2 cells do not show any granular structures stained by anti-Atx2 antibodies. Atx2-positive stress granules appear within 1 h of arsenite exposure. More distinct granules are seen after 3 h. On removing stress, the granules gradually start to clear, and after 3 h of recovery, Atx2 returns to its normal diffused state. Staining was performed using antibodies against Atx2. (B) The number of granules present per cell under control, stress (3 h), and recovery (3 h) are plotted. The number of cells and the granules present in the cells were quantified using CellProfiler. Mann–Whitney U test shows that there was a significant difference in the number of granules between stressed and recovered cells ($p < 0.05$). The ROUT method was used with coefficient Q = 1% to identify outliers and the cleaned data were used to generate the violin plot (SEM ****$p < 0.0001$). Images and raw values corresponding to the analyses are shown in Supplemental Figure S1A and Supplemental File 1. (C) Atx2 and Rin colocalize in SGs shown by staining with antibodies against Atx2 and Rin. (D) Western blotting of total cell lysates shows that eIF2α is hyperphosphorylated during 1 h (S1) and 3 h (S2) stress. Cells were allowed to recover for 3 h after both 1 h (R1) and 3 h (R2) of stress. Total eIF2α levels do not show any change. The levels of phosphorylated eIF2α and total eIF2α have been quantified for a comparison. Unpaired Student's *t* test was used for the analysis and error bars show ± SEM (*$p < 0.05$ and **$p < 0.01$). Uncropped Western blots are shown in Supplemental Figure S1B. Scale bar represents 2 µm (A) and 5 µm (C).

Strong transcriptional changes are observed after stress cessation

To identify the main differences in transcriptomes across cells at rest, under stress, and after recovery, we identified genes whose expression was altered at least $\log_2$ fold change of 2 with an adjusted *P* value (padj) <0.05 between conditions (using the average expression values across replicates in each). Of the 374 transcripts that were differentially regulated after 3 h of stress, we found that levels of 325 transcripts were elevated and only 49 reduced compared with untreated cells (Figure 2C, Supplemental File 3), indicating that stress predominantly resulted in induction of transcription.

After 3 h of recovery that is characterized by the progressive disappearance of SGs from the majority of cells, the transcriptomes of cells were even more different from untreated cells than were transcriptomes of cells 3 h after stress. Thus 1105 transcripts showed at least $\log_2$ fold change of 2 in expression in cells 3 h postrecovery compared with untreated cells. Of these 1105 transcripts, 1065 were up-regulated, and 40 transcripts were down-regulated (Figure 2C; Supplemental Figure S2Bi, ii). More detailed comparisons indicate that mRNAs up-regulated more than $\log_2$ fold change of 2 after 3 h recovery were generally induced, albeit to a lesser extent, after stress alone. Consistent with this, when transcriptomes of cells 3 h postrecovery were compared with transcriptomes of stressed cells, we found only 355 transcripts that showed a $\log_2$ fold change of 2 increase in expression after 3 h of recovery (Figure 2C; Supplemental Figure S2C). Concomitantly, we did not find any transcripts that were significantly down-regulated when transcriptomes of cells 3 h postrecovery were compared with transcriptomes of stressed cells (Figure 2C). Intriguingly, mRNAs induced by acute stress stayed up-regulated for hours after the

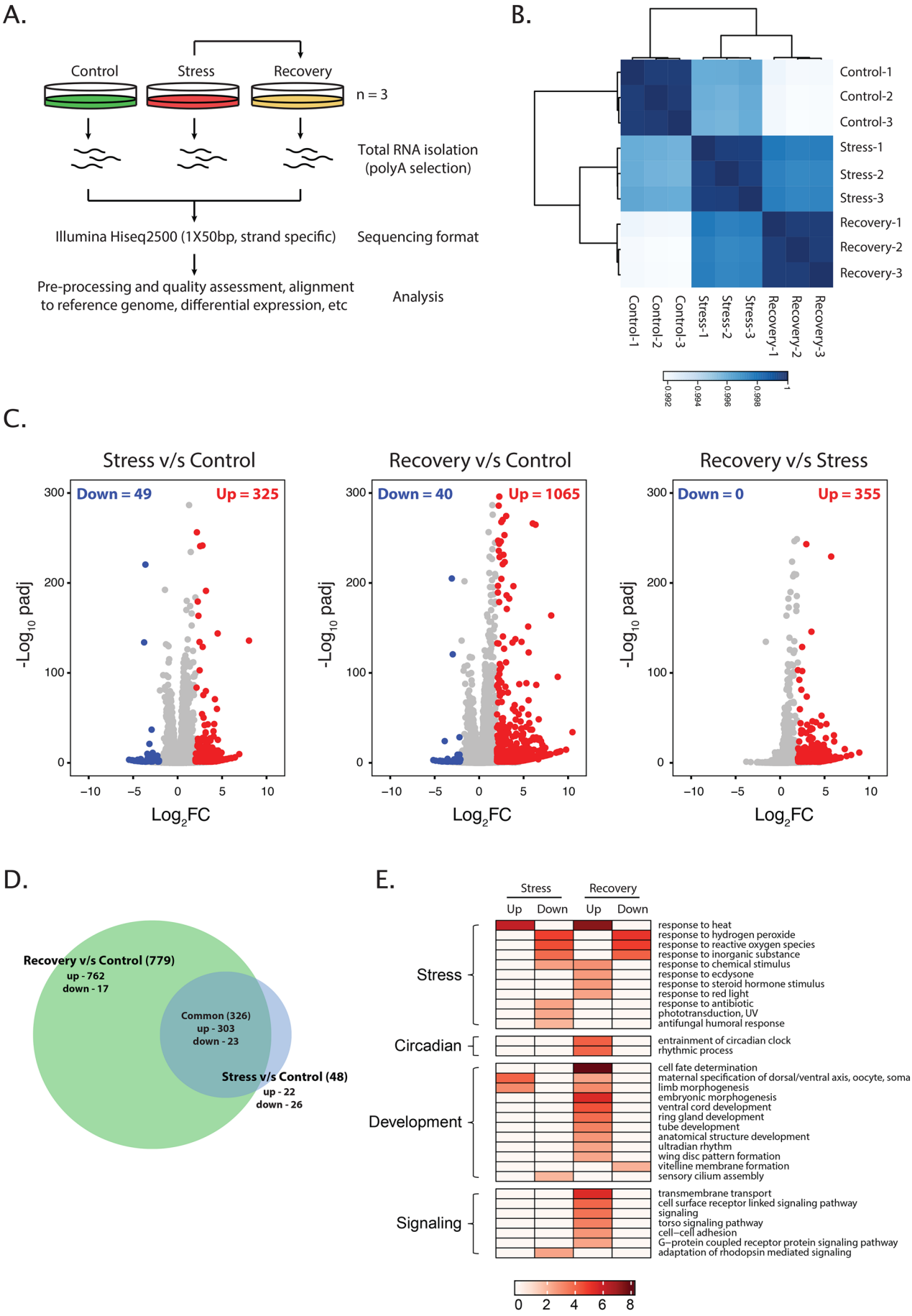
A.
Control
Stress
Recovery
n = 3
Total RNA isolation
(polyA selection)
Illumina Hiseq2500 (1X50bp, strand specific)
Sequencing format
Pre-processing and quality assessment, alignment
to reference genome, differential expression, etc
Analysis
B.
Control-1
Control-2
Control-3
Stress-1
Stress-2
Stress-3
Recovery-1
Recovery-2
Recovery-3
0.992
0.994
0.996
0.998
1
C.
Stress v/s Control
Down = 49
Up = 325
Recovery v/s Control
Down = 40
Up = 1065
Recovery v/s Stress
Down = 0
Up = 355
-Log10 padj
Log2FC
D.
Recovery v/s Control (779)
up - 762
down - 17
Common (326)
up - 303
down - 23
Stress v/s Control (48)
up - 22
down - 26
E.
Stress
Recovery
Up
Down
Up
Down
Stress
response to heat
response to hydrogen peroxide
response to reactive oxygen species
response to inorganic substance
response to chemical stimulus
response to ecdysone
response to steroid hormone stimulus
response to red light
response to antibiotic
phototransduction, UV
antifungal humoral response
Circadian
entrainment of circadian clock
rhythmic process
Development
cell fate determination
maternal specification of dorsal/ventral axis, oocyte, soma encoded
limb morphogenesis
embryonic morphogenesis
ventral cord development
ring gland development
tube development
anatomical structure development
ultradian rhythm
wing disc pattern formation
vitelline membrane formation
sensory cilium assembly
Signaling
transmembrane transport
cell surface receptor linked signaling pathway
signaling
torso signaling pathway
cell–cell adhesion
G–protein coupled receptor protein signaling pathway
adaptation of rhodopsin mediated signaling
0
2
4
6
8

stressor was removed. Thus the expression of almost all the transcripts differentially regulated in stress was also similarly altered following 3 h of post-stress recovery (Figure 2D; Supplemental Figure S2Bi and ii). Only 48 transcripts were unique to an acute stress transcriptome; 22 of these were up-regulated while 26 were down-regulated (Figure 2D; Supplemental Figure S2Bi and ii). These observations clearly show that unlike SGs, which disassemble when the stressor is removed, stress-induced transcriptional changes persist long after the stressor is gone.

A Gene Ontology (GO) enrichment analysis provided a high-level view of functional classes of genes overrepresented during stress and subsequent recovery (Figure 2E). In particular, mRNAs known to respond to increased temperature and heat stress were particularly enriched during stress and after a 3-h recovery (Figure 2E; Supplemental File 4).

Multiple classes of potentially cytoprotective mRNAs induced by stress

A detailed analysis of the identity of stress-regulated mRNAs was consistent with a model in which oxidative stress predominantly leads to the up-regulation of a cohort of genes required for a delayed response to acute stress in S2 cells (Figure 2, C and D; Supplemental Figure S3). Of 100 genes that were most strongly up-regulated after 3 h of recovery, several encoded heat-shock proteins (HSP) of the HSP70 (Hsp70Bc, Hsp70Bbb, Hsp70Ba, Hsp68), HSP40 (DnaJ-1), low molecular weight, HSP (Hsp23, Hsp26, Hsp27) families, and cochaperones (stv) families (Figure 3A). Interestingly, several of these up-regulated genes have been previously shown to be regulated by heat stress in *Drosophila* (Vos *et al*., 2016). This indicates significantly overlapping cellular mechanisms for the management of oxidative stress and heat stress, which is consistent with previous observations for the phenomenon of "cross-tolerance" in other organisms (Vert and Chory, 2011; Mittal *et al*., 2012; Perez and Brown, 2014).

In addition, we noticed a more specific up-regulation of transcripts encoding factors expected to help counter the effects of oxidative stress (Figure 3A), in particular, genes for glutathione (GSH)-S-transferases (GstD5, GstE7, GstE8, and GstS1). GSTs are detoxification enzymes that detoxify reactive oxygen species ROS) by catalyzing the addition of GSH and protect the cell from oxidative damage (Mailloux *et al*., 2013).

Apart from Hsp and GST transcripts, several noncoding (nc) RNAs, CR43481, CR45380, Uhg5, CR31044, CR43626, CR32865, Hsr-omega, and RNaseMRP:RNA were also up-regulated (Figure 3A). We speculate that these as well as up-regulated mRNAs encoding DNA-binding proteins like bab2, edl, e(y)2b, peb, Rev1, E(spl)m3-HLH, and E(spl)mbeta-HLH could potentially regulate the expression of "late" genes, such as those strongly induced after 3 h of recovery, of which several interestingly encode metabolic factors (Figure 3A; Supplemental Figure S3).

An unexpected finding is that reads corresponding to several small nucleolar RNA (snoRNA) genes that are frequent in unstressed cells are highly reduced in number both during stress and after 3 h of recovery (Figure 3B; Supplemental Figure S3B). snoRNAs are RNA PolII-transcribed, short essential non-protein-coding RNAs (60–300 nucleotides long) that are mostly localized to nucleoli (Kufel and Grzechnik, 2019; Bratkovič *et al*., 2020). The primary function of snoRNA-ribonucleoprotein complex is posttranscriptional maturation of ribosomal RNA (rRNA) and small nuclear RNAs (snRNA) through 2-O'-methylation and pseudouridylation (Bratkovič *et al*., 2020). Because most snoRNAs do not have polyA tails, it was quite surprising to find reads corresponding to snoRNAs in our polyA libraries under unstressed conditions. Since several snoRNAs are encoded in the introns of pre-mRNAs, particularly those encoding ribosomal proteins (Kufel and Grzechnik, 2019; Bratkovič *et al*., 2020), one possibility is that RNA-Seq reads for snoRNAs correspond to the introns from unspliced, polyadenylated nuclear pre-mRNAs (Supplemental Figure S3C). We therefore examined whether the reduced number of snoRNA reads after stress could correspond to increased splicing of the parent pre-RNAs.

The bed graph files for two intron-encoded snoRNAs, snoRNA:Psi18S-920 and snoRNA:Psi28S-s648 (Figure 3C), show that RNA-Seq reads corresponding to these snoRNAs are almost absent during stress and recovery. If this decrease corresponds to reduced transcription, then the parent mRNAs must also be down-regulated. Instead, the normalized counts of 11 such parent ribosomal protein genes show that in contrast to respective snoRNA reads, their levels are slightly elevated, certainly not decreased, during stress as well as after 3 h of recovery (Supplemental Figure S3C). Similarly, transcript levels of snoRNA:Me28S-A2113 and snoRNA:Psi28S-2996, which arise from RpL30 and RpL5, respectively, also show significant reduction during both stress and recovery (Supplemental Figure S3D). The most likely interpretation of these observations is that the generation of mature snoRNA present within the parent polyA mRNA through splicing becomes more efficient in response to stress, thereby enhancing their function in modifications of rRNA and snRNA, which ultimately could contribute to selective translation of oxidative stress-specific mRNAs. An alternative possibility is that snoRNAs are rapidly degraded under stress conditions, thereby altering their steady-state levels without affecting levels of the spliced parent transcripts.

Persistent transcription of chaperones after acute stress

Metabolic labeling of RNA allows one to discriminate between alterations in dynamics of RNA production or degradation (Rabani *et al*., 2011). Conventional RNA-seq does not always reflect transcriptional changes because changed levels of steady-state mRNA can also arise from altered RNA turnover (Bansal *et al*., 2020; Blatt *et al*., 2020). To determine the origin of altered transcript levels during stress and recovery as indicated by RNA seq analysis, we in vivo

FIGURE 2: Distinctive normal, stress, and recovery transcriptomes. (A) Schematic representation of the experimental design. Cells were stressed for 3 h with 0.5 mM sodium arsenite and pelleted for RNA isolation. For recovery, arsenite was removed after 3 h of stress, and cells were washed three times with S2 cell culture media and then maintained in fresh media for an additional 3 h. Cells were subsequently harvested for RNA isolation. (B) Pearson's correlation plot visualizing the correlation between samples. The color scale represents the range of correlation coefficients displayed. (C) Volcano plots showing the differentially regulated transcripts in stress and recovery with a threshold of $\log_2$ fold change of 2 with an adjusted *P* value (padj) < 0.05 between the different conditions. (D) Venn diagram showing an overlap for differentially regulated transcripts between recovery vs. control and stress vs. control. (E) GO analysis of differentially expressed genes during stress and recovery. The enriched GO terms (biological process) in differentially expressed (up/down) genes under stress and recovery conditions compared with control conditions are shown via heatmap. The scale at the bottom represents enriched GO terms in $-\log_{10}$ *p* value.

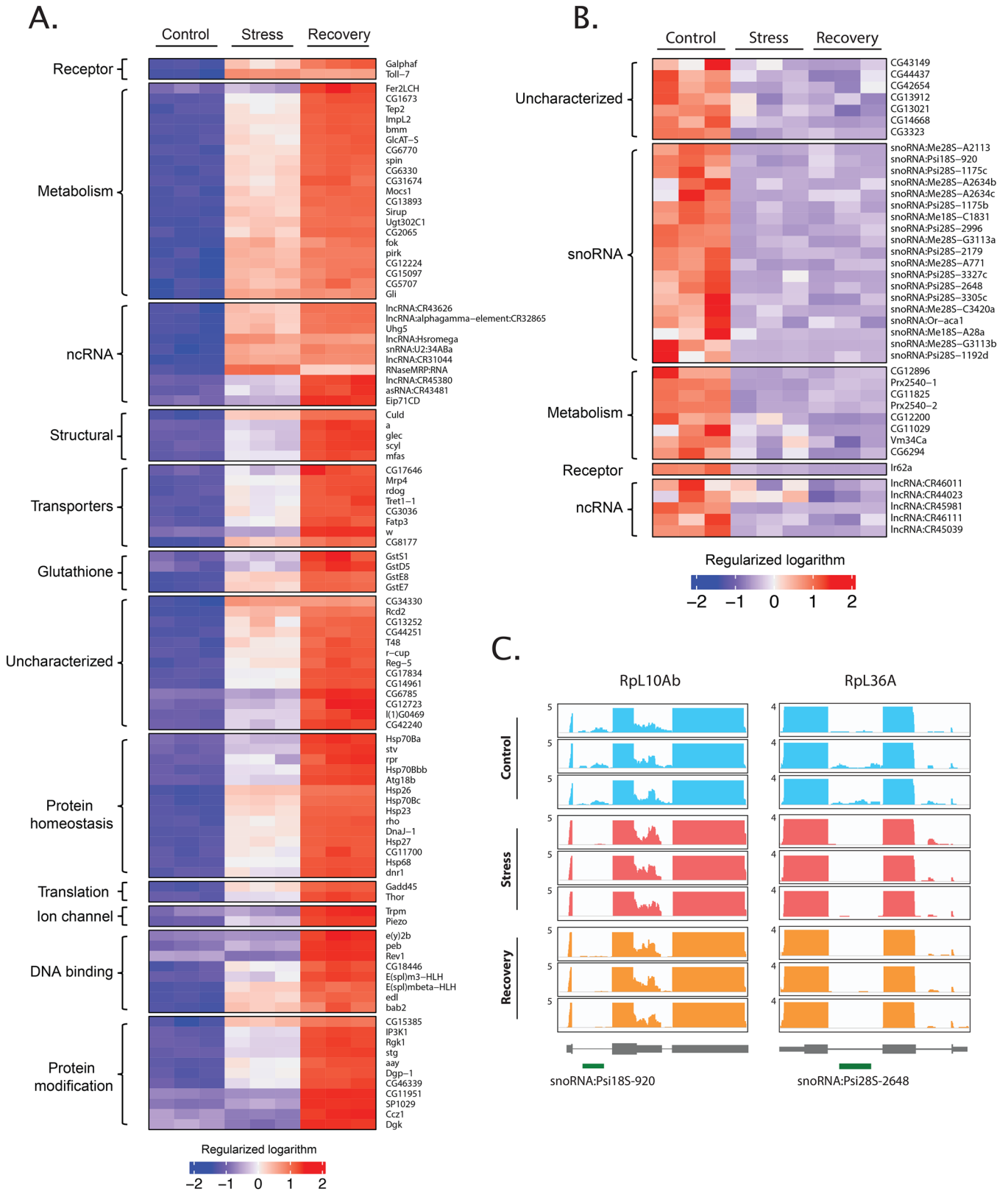

FIGURE 3: Oxidative stress results predominantly in the induction of mRNAs. (A) Heatmap for 100 genes most robustly up-regulated following 3 h of recovery from 3 h of acute stress. Genes are grouped based on predicted cellular functions. The fold induction is indicated in the color scale below. (B) Heatmap shows a smaller group of mRNAs for which reads are substantially decreased after acute stress. The color scale bar indicated fold changes represented. (C) Bed graphs showing the reads under control, stress, and recovery corresponding to the parent genes RpL10Ab and RpL36A, which harbor snoRNA:Psi18S-920 and snoRNA:Psi28S-2648.

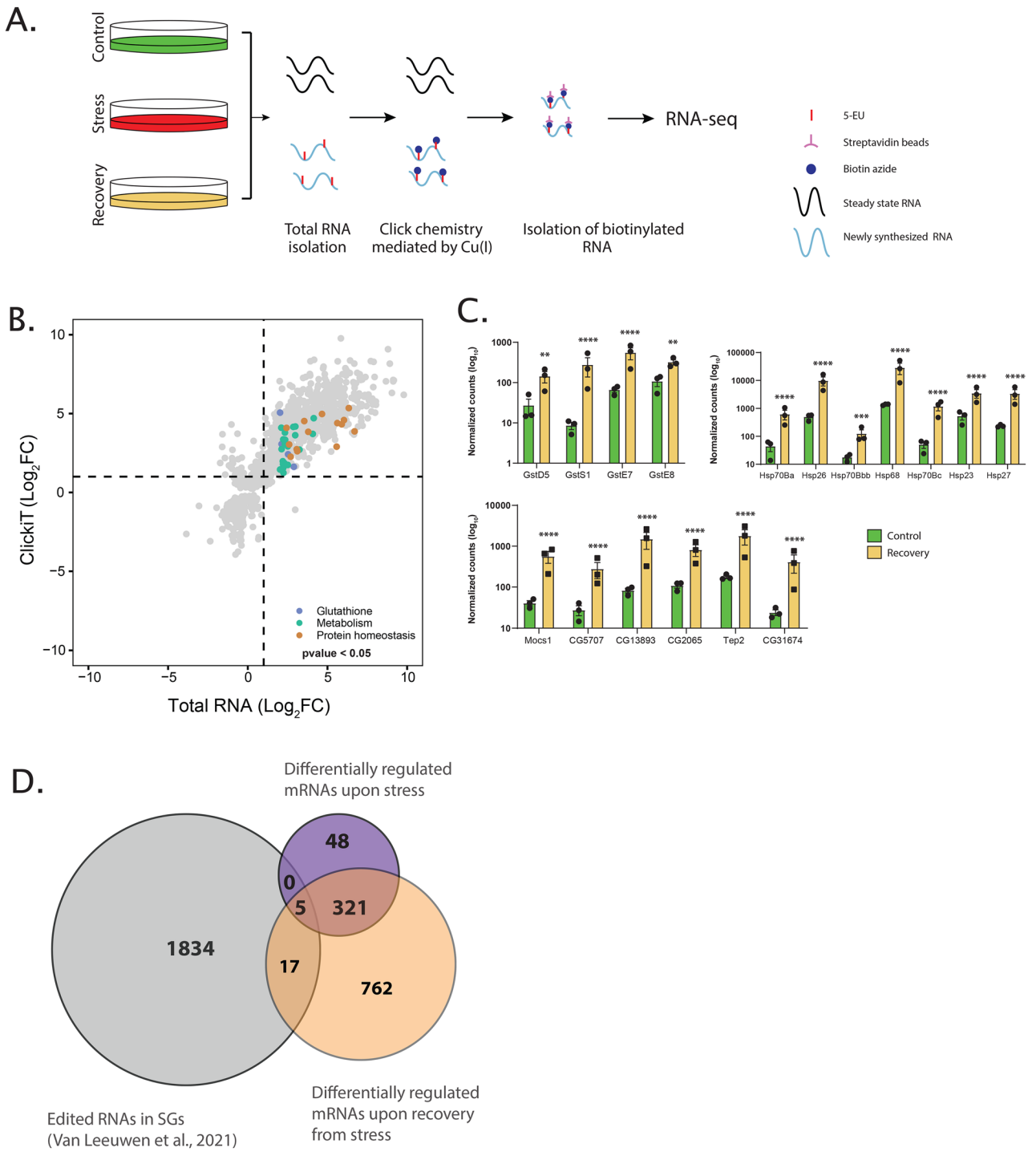

FIGURE 4: Recovery is characterized by de novo transcription. (A) Schematic for labeling mRNAs using 5-EU. (B) Enhanced levels of de novo synthesized transcripts corresponding to chaperones, GSTs, and genes involved in metabolism during recovery from stress with a threshold of $\log_2$ fold change >1.5 and p value < 0.05. (C) Normalized counts of mRNAs during recovery. Transcripts coding for GSTs, chaperones, and metabolism-related genes are shown. The error bars are represented as ± SEM with p values (**$p < 0.01$, ***$p < 0.001$, ****$p < 0.0001$) calculated using DESeq2 package. (D) Venn diagrams comparing SG transcriptome (Van Leeuwen *et al.*, 2021) with mRNAs differentially regulated in both stress and recovery.

labeled nascent mRNAs using 5-ethyl uridine (5-EU) and determined whether there was clear evidence for new transcription of "up-regulated" mRNAs using Click-iT, a technique that has been used to distinguish mRNA turnover and de novo transcription in several organisms (Jao and Salic, 2008; Chen *et al.*, 2018; Battich *et al.*, 2020; Szabo *et al.*, 2020). For control and acutely stressed cells, we added 5-EU in normal or arsenite-containing medium and collected cells after 3 h. To analyze transcription after the stressor had been removed (during recovery), we added 5-EU after 3 h of stress and then harvested the cells for RNA isolation (Figure 4A). We

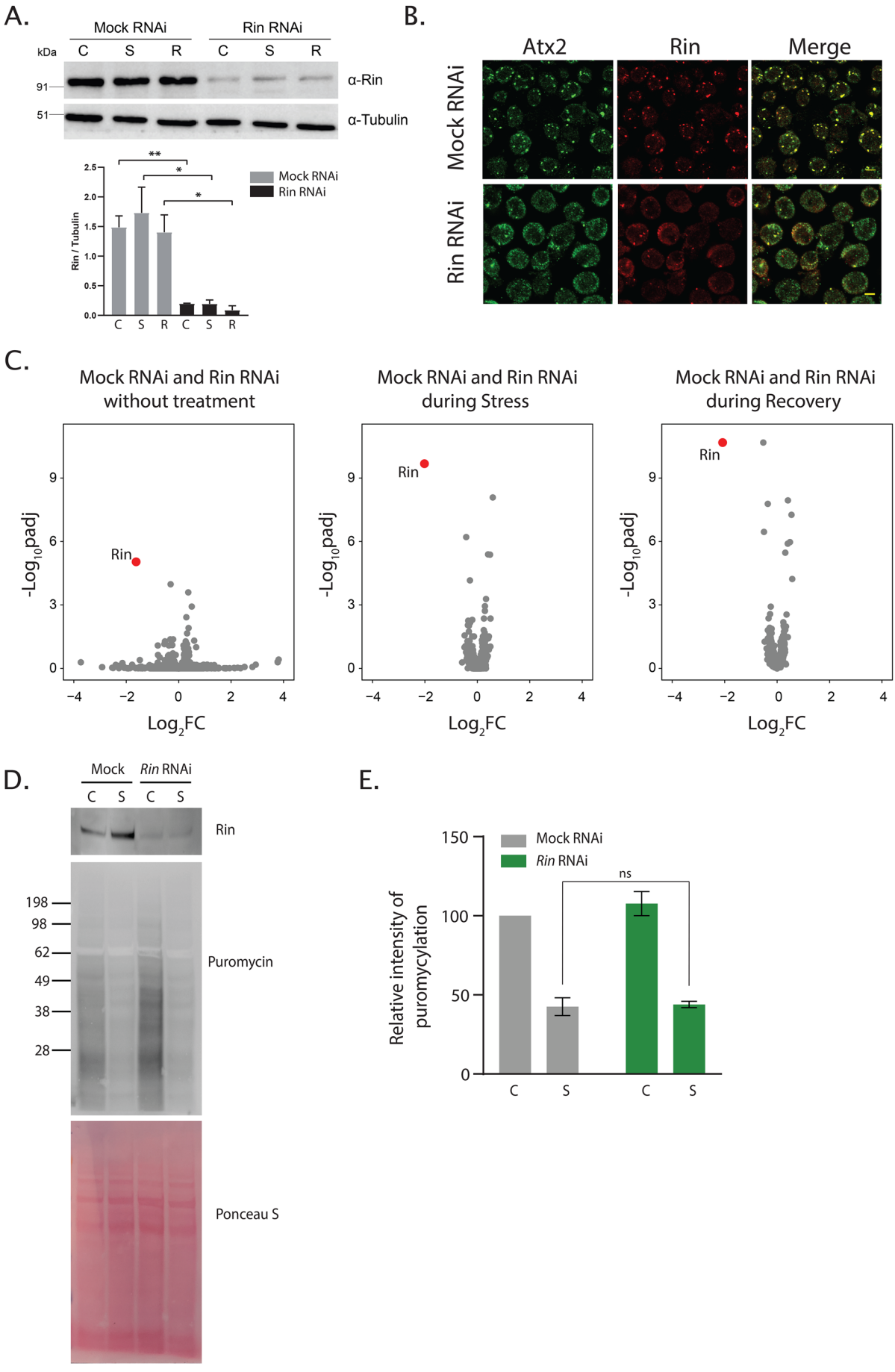
A.
Mock RNAi
Rin RNAi
kDa
C S R C S R
91
51
α-Rin
α-Tubulin
**
*
*
Mock RNAi
Rin RNAi
Rin / Tubulin
2.5
2.0
1.5
1.0
0.5
0.0
C S R C S R
B.
Atx2
Rin
Merge
Mock RNAi
Rin RNAi
C.
Mock RNAi and Rin RNAi without treatment
Mock RNAi and Rin RNAi during Stress
Mock RNAi and Rin RNAi during Recovery
Rin
-Log10padj
Log2FC
9
6
3
0
−4 −2 0 2 4
D.
Mock
Rin RNAi
C S C S
Rin
198
98
62
49
38
28
Puromycin
Ponceau S
E.
Mock RNAi
Rin RNAi
ns
Relative intensity of puromycylation
150
100
50
0
C S C S

isolated total RNA from all the samples and used the Click-iT Nascent RNA Capture kit to selectively pull down labeled nascent RNA on beads for cDNA synthesis and RNA-Seq. This method captured new transcripts without the need for them to be polyadenylated.

RNA-seq analysis of the Click-iT-captured mRNAs confirmed increased stress-induced transcription of mRNAs whose levels were elevated after stress. Transcripts coding for Hsps, for example, stv, Hsp23, Hsp26, Hsp27, DnaJ-1, Hsp70Bc, Hsp68, Hsp70Ba, etc., were seen as transcriptionally up-regulated during recovery (Figure 4, B and C; Supplemental File 5). This observation confirms that new transcription of chaperones occurs during acute stress and continues for a substantial period during recovery from stress. Interestingly, almost all the transcripts that were up-regulated in stress and recovery are predicted to be excluded from the SGs (Figure 4D). Out of the 1856 transcripts reported as present in SGs in *Drosophila* SGs (Van Leeuwen *et al.*, 2021), we found that only 5 transcripts were included among the stress-regulated mRNAs that we identified (Supplemental File 3). Similarly, only 22, corresponding to 1.2% differentially regulated transcripts in recovery, were found to be present in the reported collection of SG-associated mRNAs (Figure 4D). This comparison reveals that the mRNAs that are up-regulated during stress are excluded from SGs, suggesting that they either have roles in translational repression or encode factors that are translated during stress and recovery.

Oxidative stress transcriptional response is uncoupled from SG assembly

Given that stress induces both SGs and new transcription, we were interested to know whether the assembly of SGs contributed to signaling transcription of at least a significant subset of target mRNAs, as has been proposed following viral infection (Tsai and Lloyd, 2014; McCormick and Khaperskyy, 2017; Alam and Kennedy, 2019). To address this outstanding question, we asked how disrupting SG assembly would affect stress-induced transcription.

We used dsRNA-mediated RNAi to knock down the levels of *Rin* in S2 cells and independently assessed the effect of this perturbation on SG granule assembly as well as on stress-induced transcription. Experimental cells treated with dsRNA targeting endogenous Rin mRNA showed reduced levels of Rin protein compared with mock control cells (treated with dsRNA targeting GFP) (Figure 5A). In mock control cells, arsenite exposure robustly induced Atx2- and Rin- containing SGs (Figure 5B). In contrast, and as predicted, *Rin*-RNAi treated cells with reduced *Rin* mRNA and protein (Figure 5A) were unable to form SGs (Figure 5B). To test whether the inability to form SGs affected the transcriptional response to stress, we used RNA-seq to determine and analyze transcriptomes in mock and *Rin* RNAi cells exposed to arsenite as described previously (Figure 2A). Transcriptomes for three control and three *Rin* RNAi replicates showed high internal correlation coefficients within each group (between 0.992 and 1.0), demonstrating high similarity among biological replicates within each condition (Supplemental Figure S4A). However, and remarkably, similar levels of correlation were also seen across groups: indeed, mock and *Rin* RNAi transcriptomes were largely indistinguishable (Supplemental Figure S4A). This observation suggests that *Rin* knockdown, which prevents normal SG formation, has no significant effect on stress-induced transcription. Consistent with this, i) transcriptomes of *Rin*-deficient cells following 3 h of arsenite exposure matched most closely with those of mock RNAi cells after 3 h of acute stress (Figure 5Cii), and ii) transcriptomes of *Rin*-deficient cells 3 h poststress recovery matched most closely with those of similarly treated mock RNAi cells (Figure 5Ciii).

Further, volcano plots comparing mock and *Rin* RNAi transcriptomes showed that the transcript levels for all genes remained mostly unchanged following *Rin* knockdown, with the notable exception of *Rin* itself, which was reduced almost fourfold compared with the levels in mock RNAi (Figure 5C; Supplemental Figure S4B). The selective effect on *Rin* also confirmed that the effect of *Rin* RNAi was target-specific, with no significant off-target effects. A comparison of the top 100 differentially regulated genes showed no difference among the mock and *Rin* RNAi cells (Supplemental Figure S4C; Supplemental File 6). These observations suggest that oxidative stress-induced SGs do not have a role in oxidative stress-induced transcription, and they appear to be independent but parallel pathways.

It was notable that neither stress nor *Rin* knockdown had any significant effect on the expression of mRNAs encoding known stress-granule or stress-granule-associated RNA-binding proteins within the timescale of our experiments. Thus there were no significant changes in the transcript levels for Atx2, Caprin, Cabeza (Fus), Fmr1 (FMRP), Me31B, Pontin (RuvBL1), Reptin (RuvBL2), Ref(2)p (p62/SQSTM1), Rox8 (TIA1), TBPH (TDP43), and Lingerer (UBAP2L) (Supplemental Figure S4B).

We also used O-propargyl-puromycin incorporation assays to examine whether global translational repression induced by stress was affected under conditions where Rin levels are low, and SGs are not observed. Strikingly, under conditions of reduced levels of Rin

FIGURE 5: *Rin* knockdown prevents SG assembly without altering stress-induced transcription. (A) Western blot analyses using total cell lysates from mock RNAi and *Rin* RNAi cells under control, stress, and recovery show drastically reduced Rin protein levels in *Rin* RNAi cells. Tubulin was used as a loading control. Anti-Rin (1:500) and anti-tubulin (1:4000) antibodies were used. The levels of Rin have been quantified for comparison. Unpaired Student's *t* test was used for the analysis and error bars show ± SEM (*$p < 0.05$ and **$p < 0.01$). (B) Arsenite does not cause SG induction in Rin/G3BP deficient cells (after Aguilera-Gomez *et al.*, 2017). On stress, both Atx2 and Rin colocalize in granules in mock RNAi cells (i–iii). However, in *Rin* RNAi cells, no granules are assembled on stress, and Atx2 is diffusely distributed (i'–iii'). Scale bars represent 5 µm. Anti-Atx2 (1:500) and anti-Rin (1:500) antibodies were used for immunofluorescence. (C) Volcano plots showing the similarity in transcriptomes across mock RNAi and *Rin* RNAi samples with $\log_2$ fold change = 1.5 and adjusted *P* value < 0.05. The red dot indicates the levels of Rin in *Rin* RNAi samples. (D) O-propargyl-puromycin incorporation assays in mock and *Rin* RNAi cells. Western analyses using total cell lysates from mock RNAi and *Rin* RNAi cells under control and stress conditions were used for puromycin incorporation. Anti-puromycin and Anti-Rin antibodies were used at 1:1000 and 1:500 dilutions, respectively. A representative blot of four independent experiments is shown. Ponceau S staining depicts the protein levels in the different cell lysates. (E) Bar graphs showing the relative intensity of puromycylation in mock RNAi and *Rin* RNAi cells under control and stress conditions. Mann–Whitney U test shows that there was no significant difference in puromycylation between mock RNAi stress and *Rin* RNAi stress cells. Error bars show ± SEM (ns $p > 0.05$).

where SGs do not form, global translation is still inhibited by stress (Figure 5, D and E). This is consistent with previous work in mammalian cells, suggesting that although the translation is widely repressed during stress, only ~5% of mRNA is sequestered within SGs (Khong *et al*., 2017). Interestingly, levels of Rin showed an increase during stress in mock cells treated with puromycin which further points to another layer of complexity (Figure 5D).

DISCUSSION

The interrelationship between SGs and transcriptional response to oxidative stress

Given the importance of SGs and oxidative stress in physiology and disease, research has not been undertaken to study how these two cellular phenomena, namely, SGs and oxidative stress-induced transcription, influence each other in metazoa (Zou *et al*., 2000; Brown *et al*., 2014; Wolozin and Ivanov, 2019; Asadi *et al*., 2021). However, extensive work in bacteria, plants, and yeast as well as some in metazoan animal species has provided important insights independently (Wohlbach *et al*., 2009; He *et al*., 2018; Reichmann *et al*., 2018; Blevins *et al*., 2019). Global transcriptional changes that occur during recovery following stress remain relatively sparsely studied (Sørensen *et al*., 2005). First, different types of stresses can induce expression of overlapping groups of genes, pointing to the principle of cross-tolerance, wherein proteins induced by and that confer protection to heat stress, for instance, may also be similarly regulated and perhaps protective during oxidative stress (Morimoto, 1998; Jacobson *et al*., 2012; Dahl *et al*., 2015; Chowdhary *et al*., 2019). This could, in part, be explained by overlapping cellular effects of stressors: both heat and oxidative stress alter protein folding, and chaperone systems that prevent protein aggregation or promote refolding may be required in both conditions. Moreover, stress-responsive genes could also encode conserved proteins involved in constitutive cellular maintenance (Kültz, 2003; Rebeaud *et al*., 2020).

Specific suites of genes (and functions) induced by and required under oxidative stress

The induction of oxidative stress by arsenite generates ROS in the cell, which regulates many stress regulators, including HSPs (Ruiz-Ramos *et al*., 2009). The up-regulation of *Hsp* mRNAs seems to be an evolutionarily conserved response required for folding the misfolded/aggregated proteins during stress, aging, as well as during development (Michaud *et al*., 1997; Zou *et al*., 2000; Ruiz-Ramos *et al*., 2009; Colinet and Hoffmann, 2010; Colinet *et al*., 2010; Verghese *et al*., 2012; Brown *et al*., 2014; Vos *et al*., 2016). In *Drosophila*, *Hsps* are also induced during recovery from cold stress (Colinet *et al*., 2010; Štětina *et al*., 2015); however, the type of HSPs and the amount of HSPs induced depend on the type of stress (Morano *et al*., 2012; Zhao *et al*., 2015). We find a similar up-regulation of *Hsp* mRNAs during stress (Supplemental Figure S3A) as well as during recovery (Figure 3). Intriguingly, the up-regulation of mRNAs during recovery was via active transcription as seen by metabolic labeling (Figure 4B) and not because of the enhanced stability of mRNAs during recovery. This is a significant finding as it implies that the *Hsp* coding mRNAs, which are up-regulated during stress, may have separate functions than those up-regulated during recovery, just like it has been shown for HSP70 in thermotolerant cells (Tian *et al*., 2021). The up-regulation of small HSPs (sHSPs; Hsp20/α-crystallin family) and HSP70 mRNAs on oxidative stress suggests extensive misfolding of proteins under these conditions, which needs to be managed such that they can be refolded into the native state for the cell to recover. sHSPs function as "holdases" and prevent the formation of denatured protein aggregates in the cell and while HSP70s are the main folding agents of nascent polypeptide chains as well as for misfolded proteins during periods of stress (Finka *et al*., 2016; Vos *et al*., 2016).

Akin to chaperones, GSTs also have a cytoprotective function; for example, they can protect against oxidative damage to DNA and prevent mutations (Veal *et al*., 2002; Allocati *et al*., 2018). As seen for *Hsp* mRNAs, we find that several GST mRNAs are up-regulated both during stress (Supplemental Figure S3A) and are actively transcribed during recovery (Figures 3A, 4B). In yeast, it is known that GSTs are required for cellular resistance to oxidative stress (Veal *et al*., 2002). There is also the interesting possibility of GSTs being regulators of stress kinases and thus modulating signal transduction (Adler *et al*., 1999; Laborde, 2010). Up-regulation of transcripts encoding for proteins involved in such cytoprotective functions points to the fact that to attain homeostasis during recovery, a cell needs to prevent protein aggregation (by the action of sHSPs), fold/refold, misfolded proteins (by a harmonious action of HSP70s and HSP40s), and get rid of free radicals generated due to oxidative stress (by synthesizing more GSTs).

Similar to the coding genes, aberrant up-regulation of several ncRNAs is observed during stress and disease conditions (Brown *et al*., 2014; Torrent *et al*., 2018; Connerty *et al*., 2020). We find that several ncRNAs are up-regulated during stress and recovery, the prominent ones being Hsr omega and RNaseMRP:RNA (Figure 4). During stress, rRNA processing might be affected, and up-regulation of RNaseMRP:RNA might be a counteractive response during stress. ncRNAs can likely regulate the stability of mRNAs as they bind to several different proteins and modulate their activity by sequestering them away from their sites of action (Lakhotia, 2012). LncRNAs can also act as a sponge for microRNAs, preventing the cleavage of mRNAs whose translation is required during stress and recovery, as well as regulate translation because of complementarity (Lee and Rio, 2015). Although mature Rpl13a mRNA levels are not affected, oxidative stress reportedly leads to up-regulation of intronic C/D box snoRNAs present in the *Rpl13a* gene that is required for propagation of oxidative stress whilst their loss affected mitochondrial metabolism and lowered ROS (Michel *et al*., 2011; Lee *et al*., 2016; Ly *et al*., 2017). Akin to the above observation, we also found several snoRNA transcripts significantly reduced during stress and recovery. These studies imply that the differentially regulated snoRNAs might be crucial for oxidative stress response in *Drosophila* cells as well. Several other snoRNAs are also involved in alternative splicing of mRNAs (Kishore and Stamm, 2006; Kishore *et al*., 2010; Falaleeva *et al*., 2016; Bratkovič *et al*., 2020). It is thus obvious to speculate that the levels of a set of snoRNAs might be regulated via their splicing while another set of snoRNAs might be involved in promoting alternative splicing of mRNAs.

General and specific features of the oxidative stress transcriptome in flies

In the current study, we provide an overview of the global transcriptional changes in *Drosophila* S2 cells on exposure to sodium arsenite stress and subsequent recovery. The results reveal a general increase in the transcription of *Hsp* genes during both stress and recovery, accompanied by increased transcription of genes coding for detoxifying enzymes and several ncRNAs. We also show that knockdown of *Rin* prevents the assembly of SGs during stress and that oxidative stress-induced transcriptional alterations are a completely independent but parallel event with respect to SG assembly. The number of transcripts that is differentially regulated during recovery is almost three times more than that in stress. The 3 h recovery is short and the transcriptome may reflect early recovery genes

that belong to several different classes of proteins as compared with the stress, where the transcripts mainly belong to genes coding for proteins involved in stress response or proteolysis. Interestingly, we did not find any genes that underwent significant down-regulation during recovery while the up-regulation of several transcripts involved in the development and metabolic processes during recovery underlines the efforts being made by the cell to restore homeostasis.

Significance of analysis of acute stress and recovery transcriptomes and potential functions for specific classes of genes identified

The transcriptional up-regulation of various types of chaperones (Figure 3A; Supplemental Figure S3A) suggests that apart from their protein folding role, these proteins are also crucial for preventing promiscuous interactions among aggregation-prone proteins by promoting the formation of SGs (Gong and Golic, 2006; Gitter *et al.*, 2013; Štětina *et al.*, 2015). The chaperones could modulate SG formation and disassembly (Ganassi *et al.*, 2016; Alberti *et al.*, 2017; Mateju *et al.*, 2017). HSP70 has also been found to be present in the cores of ring-shaped TDP43 annuli in neurons (Yu *et al.*, 2021). HSP27 prevents the entrance of FUS into SGs, suggesting that HSP27 may be necessary for the stabilization of the dynamic phase of SGs (Liu *et al.*, 2020). HSP27 has also been shown to bind polyubiquitin chains and interact with 19S proteasome (Bozaykut *et al.*, 2014; Mogk *et al.*, 2019), suggesting elevated levels of this protein during recovery may also play a role in protein triage. HSP67BC, another small HSP, has been implicated in preventing toxic protein aggregates in *Drosophila* in a HSP70-independent manner (Vos *et al.*, 2016). Similarly, the yeast HSP40s, Ydj1, and Sis1 are important for the disassembly of SGs (Walters *et al.*, 2015). Up-regulation of specific chaperone mRNAs during recovery (Figure 3A) and the concomitant dissolution of arsenite-induced SGs can be likened to the clearance of protein aggregates achieved by overexpression of specific HSPs (Warrick *et al.*, 1999; Chan *et al.*, 2000; Huen and Chan, 2005; Vos *et al.*, 2016; Webster *et al.*, 2019; Vendredy *et al.*, 2020). In fact, pharmacological activation of HSP70 has been shown to ameliorate neurotoxicity caused by aiding the clearance of polyglutamine aggregates (Wang *et al.*, 2013). Up-regulation of transcripts of both ATP-dependent and -independent HSP mRNAs (Figure 4, B and C) might implicate a cellular strategy wherein a cell can employ these proteins in clearing aggregates distinctly and more efficiently (Fare and Shorter, 2021); some of these genes may also be involved in long-term stress adaptation (Bijlsma and Loeschcke, 2005; De Bruijn, 2016).

SG assembly contributes minimally to the transcription of oxidative stress-induced genes

If SG formation is essential for the cellular stress response, blocking its formation should affect the cellular stress response (Lee *et al.*, 2020). Apart from their role in blocking cellular translation, SGs are also known to stimulate transcription of interferons in response to viral infections, suggesting that SGs may modulate transcription indirectly (Tsai and Lloyd, 2014; McCormick and Khaperskyy, 2017). The SG protein Rin/G3BP is a primary nucleator of SGs whose knockdown prevents SG assembly in response to starvation in *Drosophila* S2 cells (Aguilera-Gomez *et al.*, 2017) as well as during several other conditions in different mammalian cell lines (Lee *et al.*, 2020; Sanders *et al.*, 2020; Yang *et al.*, 2020). Apart from its role in SG assembly, the housekeeping functions of Rin/G3BP involve binding to RNA and regulating selective protein synthesis during oxidative stress via mRNA partitioning (Laver *et al.*, 2020; Somasekharan *et al.*, 2020). We also find that lowering the levels of Rin, thereby preventing SG formation, had no effect on the inhibition of global translation in S2 cells during stress (Figure 5D). In yeast cells that were deficient in forming SG in response to heat stress, enormously high levels of mRNAs coding for the HSPs (*HSP12* and *HSP104*) and significantly lower levels of genes involved in rRNA processing, part of the RiBi regulon (*PWP1, UTP13,* and *DIP2*) were found (Yang *et al.*, 2014). The authors opined that this increase or decrease in specific mRNAs levels could be due to alteration in transcription kinetics or altered mRNA stability. In contrast, we find that lowering levels of Rin, hence inhibiting the formation of SGs, does not affect transcription under stress (Figure 5). This is surprising because Rin has several housekeeping functions apart from being essential for SG condensation, but it may also not be required in specific cells; for example, TDP43 can form aggregates that do not contain G3BP/RNAs and thus do not require the formation of SGs (Pazman *et al.*, 2000; Baumgartner *et al.*, 2013; Kedersha *et al.*, 2016; Gasset-Rosa *et al.*, 2019; Buddika *et al.*, 2020; Guillén-Boixet *et al.*, 2020; Laver *et al.*, 2020; Sanders *et al.*, 2020; Yang *et al.*, 2020). Strikingly, comparative transcriptome analysis between mock and *Rin* RNAi cells revealed no change in the type of differentially regulated transcripts nor any significant alterations of fold changes in expression of individual mRNAs during stress and recovery (Figure 5). The differentially regulated transcripts in stress and recovery are also excluded from SGs (Figure 4D), which also implies that the arsenite-induced SG assembly and transcriptional alterations are parallel but independent events. There might be several underlying layers of cellular intricacies that might link these two events.

Transcription of stress-responsive genes serves a crucial role in implementing a rapid and robust stress response (Vihervaara *et al.*, 2017, 2018). On stress removal, the SGs dissolve, and cap-dependent translation begins as suggested by the loss of eIF2α phosphorylation; however, if these recovery responses are attributed to the reversal of transcriptional changes that had occurred during stress it is not known (Figure 6). Further, if transcriptional dysregulation during recovery plays any role in SG dissolution it remains unknown. Ultimately, comparing stress and recovery responses as a continuum but not in isolation is crucial in dissecting these two phenomena with exact opposite consequences to cellular homeostasis.

We propose that alterations in oxidative transcriptional response are a cellular response against acute stress. At the same time, the assembly of SGs is an immediate effect to counter stress (Figure 6). However, it remains to be elucidated: what is the involvement of the genes that are differentially regulated during recovery on the dissolution of SGs? Since *Rin* RNAi cells do not form visible SGs, it raises several important questions: i) although mRNA is devoid of ribosomes, what is their fate? ii) What is the status of the global proteome when SG assembly has been prevented? Further studies need to be undertaken to address these questions.

MATERIALS AND METHODS

Request a protocol through *Bio-protocol*.

Cell culture and treatments

Drosophila S2R+ cells were obtained from DGRC and cultured in the semiadhering state in Schneider's medium (S2 medium) with 10% fetal bovine serum, penicillin, and streptomycin at 25°C. Cells were maintained at 50% confluency in fresh S2 media for at least 24 h before being used for stress experiments.

To induce stress, cells were subjected to 0.5 mM sodium arsenite in S2 media for 3 h at room temperature on a rocking shaker. After

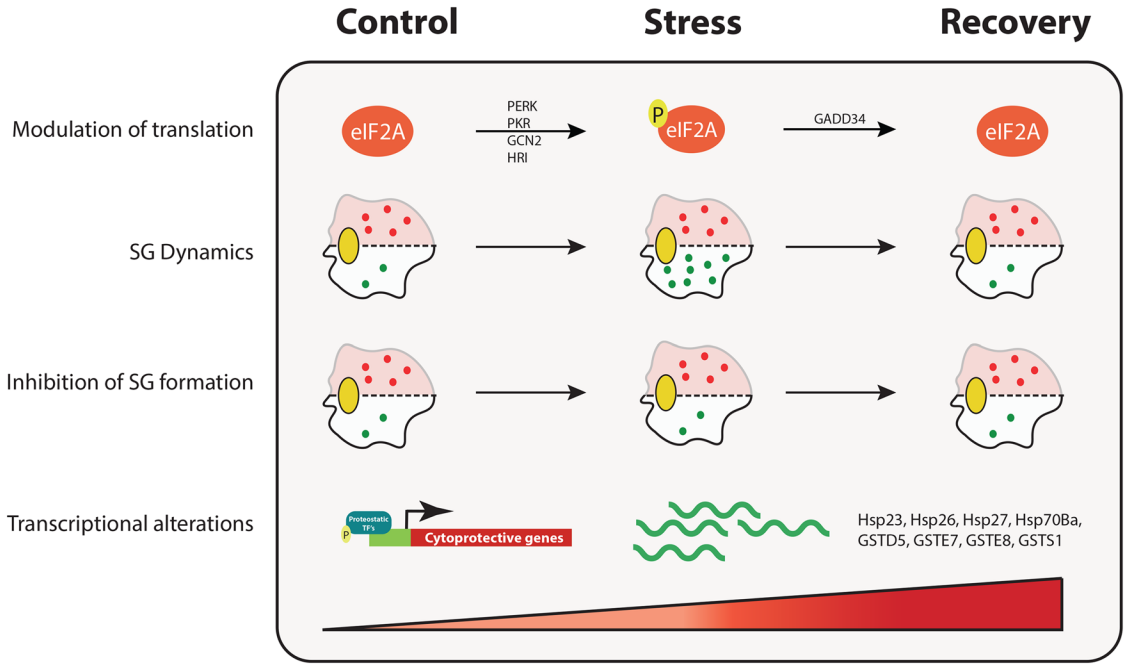

FIGURE 6: A model depicting the various cellular changes taking place during stress and subsequent recovery. eIF2α gets phosphorylated at serine 51 during stress by the action of any of the four kinases, leading to a block in cap-dependent translation. On the removal of stress, phosphorylation is lost, and cap-dependent translation is restored. This is concomitant with assembly and clearance of SGs, respectively, during stress and recovery, as well as with increased transcription of cytoprotective genes such as HSPs and GSTs mediated by proteostatic transcription factors (HSF1, FOXO, NRF2, etc). However, when the formation of SG is prevented by lowering down levels of Rin, there is no change in the transcription of the cytoprotective genes. The cells reflect two cellular states: i) the upper half depicts pathological conditions evident with the presence of persistent granules formed by proteins (such as TDP43 [Gasset-Rosa *et al.*, 2019], Htt [Huelsmeier *et al.*, 2021]) which are assembled in a SG-independent way and do not contain RNA or canonical SG proteins; ii) the lower half represents a healthy cell that assembles and disassembles SGs dynamically. Green dots represent SGs while red dots show pathological granules.

3 h, arsenite containing S2 media was removed by centrifugation at 2000 rpm for 5′, and the cells were washed three times with fresh media and kept for recovery in fresh complete S2 media. Recovering cells were kept on the rocking shaker for an additional 3 h at room temperature.

For labeling with 5-EU, 200 µm EU were added as indicated in Figure 4A. Briefly, for labeling transcripts under control and stress conditions, 5-EU either in a normal medium or in a medium containing 0.5 mM sodium arsenite. Cells were then washed and harvested for RNA isolation. For labeling transcripts during recovery, cells were initially stressed with 0.5 mM sodium arsenite for 3 h and then washed three times with fresh S2 media; 5-EU was added at the start of the 3 h recovery period, after which cells were harvested for RNA isolation.

RNA isolation and RNA Seq

After stress and recovery, RNA was isolated using TRIzol reagent (Invitrogen, USA) as per the manufacturer's protocol. RNA concentration was measured using a Qubit RNA assay kit in Qubit 2.0 Fluorometer (Life Technologies, USA). RNA integrity was confirmed using the RNA Nano 6000 assay kit of the Bioanalyzer 2100 system (Agilent Technologies, USA). Poly(A)-enriched mRNA library was made using TruSeq RNA Library Preparation Kit V2 (RS-122-2001) and sequenced using HiSeq SR Rapid Cluster Kit v2 (GD-402-4002) to generate 1 × 50 single-end reads on Illumina HiSeq2500 sequencing platform.

In silico analysis

For transcriptome analysis, all sequencing reads obtained post adaptor removal had a mean quality score (Q-Score) > = 37, so no trimming was required. All the further downstream analyses were performed on this high-quality data. For read mapping, the reference genome and gene model annotation files of *Drosophila melanogaster,* version dm6, were downloaded from the UCSC genome browser. Single-end processed reads were aligned to the reference genome using STAR v2.5.3 with default parameters. HTSeq-count v0.11.2 and the "-s reverse" option were used to count the read numbers mapped to each gene before differential gene expression analysis. Differential gene expression among samples was performed using the DESeq2 package. The data are available with the assigned GEO accession # GSE178464. For GO analysis of differentially expressed genes under stress and recovery, enriched GO terms with <0.05 *P* value were identified using BINGO plug-in at Cytoscape (v.3.8.0) and the enriched GO terms were shown in heatmap via MeV (v.4.9.0).

The number of granules per cell were quantified using CellProfiler (https://cellprofiler.org/). Nuclear staining with DAPI was used to mark and count the number of cells while Rox8 was used as a granule marker. Thresholding in signal intensity in the range of 0.2–1.0 was used to select and count the granules. 100–150 cells per field and two such fields were analyzed after which the raw cell counts and granule counts were tabulated. Outliers were identified and removed using the "Identify outliers" function in GraphPad

Prism 9. The ROUT (Robust regression and outlier removal) method was used with a coefficient Q = 1%. This defines the stringency of outlier removal. The cleaned data were then used to plot the points in the form of a violin plot, and Mann–Whitney statistics were carried out (error bars show ± SEM, ****$p < 0.0001$).

Immunostaining and fluorescence

Immunostaining was performed as described earlier (Bakthavachalu *et al.*, 2018). Briefly, S2R+ cells were grown in T25 flasks to almost 70–80% confluency. Stress and recovery experiments were performed as described above. Cells were fixed with 4% paraformaldehyde for 10 min, followed by permeabilization with 0.05% Triton-X-100 for 10 min. This was followed by blocking with 1% bovine serum albumin for 30 min. The cells were then incubated with antibodies against Atx2 (1:500), Rox8 (1:1000), and Rin (1:500), followed by probing with 1:1000 dilution of Alexa Fluor 488, 568, and 647 (Abcam) secondary antibodies, respectively. Confocal imaging was done using the PALPON 60×/1.42 oil objective of the Olympus FV3000 microscope. Images were processed using ImageJ software.

Double-stranded (ds) RNA generation

Mock and *Rin* RNAi were performed using dsRNA produced by in vitro transcription (IVT). For mock, we utilized GFP open reading frame as the target site. RNAi target sites were chosen using the SnapDragon tool (https://fgr.hms.harvard.edu/snapdragon) (Hu *et al.*, 2017). PCR-generated DNA templates containing the T7 promoter sequence at both ends were used as IVT template for dsRNA synthesis using Megascript T7 High Yield Transcription kit (Invitrogen). The primer details are provided in Supplemental File 7.

dsRNA transfection into cells for RNAi experiments

Wild-type *Drosophila* S2 cells were depleted for *Rin* mRNA by dsRNAi. Briefly, 0.5 million cells were transfected with 5 µg of dsRNA. After 48 h of the first round of transfections, cells were again transfected with 5 µg of dsRNA. After 96 h of the first transfection, cells were analyzed for the knockdown of Rin using Western blotting, and RNA was isolated using TRIzol reagent (Invitrogen) as per the manufacturer's protocol. Illumina library was prepared from Poly(A)-enriched mRNA using TruSeq RNA Library Preparation Kit V2 (RS-122-2001) and sequenced using HiSeq SR Rapid Cluster Kit v2 (GD-402-4002) to generate 1 × 50 single-end reads.

For puromycylation assays, after 93 h of mock and *Rin* dsRNA transfections, stress was induced as previously described above. Puromycin was added during the final 15 min at a final concentration of 4 µg/ml. Cells were then immediately harvested and analyzed for the knockdown of Rin and for puromycin incorporation.

Protein isolation and Western analysis

Mock RNAi and *Rin* RNAi cells were maintained, stressed, and recovered as mentioned above. Total protein isolation was performed as described earlier (Sudhakaran *et al.*, 2014). Briefly, 0.2 million cells were pelleted and resuspended in 50 µl lysis buffer (25 mM Tris HCl [pH 7.5], 150 mM NaCl, 10% [vol/vol] glycerol, 1 mM EDTA, 1 mM dithiothreitol, 0.5% Nonidet P-40, and complete protease inhibitor tablets from Roche) and incubated at 4°C for 30 min with intermittent vortexing. The lysate was then spun at 4°C at 13,000 rpm for 30 min. The supernatant was collected, and protein was quantified using Nanodrop. For puromycylation, cells were lysed and normalized for protein concentration using the Bio-Rad Protein Assay Kit (Bio-Rad Laboratories, # 5000001) and a spectrophotometer. Western blotting was performed using rabbit anti-Rin (1:1000), rabbit anti-phospho-eIF2α (1:1000, 9721L CST), rabbit anti-eIF2α (1:1000, SAB4500729-100UG), mouse anti-puromycin (1:2000, MABE343 Sigma-Aldrich), and mouse anti-tubulin (1:4000, E7c DSHB). Goat anti-rabbit HRP (sc-2004) and goat anti-mouse HRP (sc-2005) HRP–conjugated secondary antibodies were used at 1:10000 dilution.

The band intensities for p-eIF2α under various treatments were acquired by measuring the mean gray value in ImageJ (https://imagej.net/software/fiji). Eight-bit images were used for quantification and hence the mean gray values were subtracted from 255 (which corresponds to the number of pixels) to obtain inverted pixel densities. Background subtraction was performed to eliminate nonspecific signals and the resultant values were then normalized to the corresponding numbers obtained for total eIF2α. The same protocol was followed to quantify the levels of Rin in mock RNAi and *Rin* RNAi cells except that the normalization was done against the levels of tubulin. GraphPad Prism 9 (https://www.graphpad.com/) was used to plot the normalized values as a bar plot and unpaired Student's *t* test was used for statistical analysis ($p < 0.05$).

ACKNOWLEDGMENTS

We thank K. VijayRaghavan for his valuable feedback and suggestions during the course of this work. We also thank the members of the Ramaswami and Bakthavachalu labs, as well as Roy Parker (HHMI and University of Colorado Boulder) for useful discussions and/or comments on the manuscript. We thank Elizabeth Gavis (Princeton University, NJ) and Nicholas Sokol (Indiana University, IN) for sharing Rasputin and Rox8 antibodies with us. We acknowledge Drosophila Genomics Resource Centre (supported by National Institutes of Health Grant 2P40OC010949) for *Drosophila* S2 cells. The work was supported by a Science Foundation Ireland (SFI) Investigator grant to M.R. and an Irish Council Postgraduate Fellowship to G.T. The work is partly supported by the DBT/Wellcome Trust India Alliance Fellowship (IA/I/19/1/504286) awarded to B.B., who is also a recipient of the SERB-STAR award (STR/2020/000056). We acknowledge the support from INSA Young Scientist Project (INSA/SP/YSP/143/2017) (A.S.), from SERB to M.R. from a collaborative VAJRA award to Raghu Padinjat, and a CSIR fellowship (D.J.). We thank Awadhesh Pandit from the NCBS NGS facility for help with RNA-seq and Raghu Padinjat for hosting AS at NCBS. We also thank CIFF at NCBS for imaging facility.

REFERENCES

Adler V, Yin Z, Fuchs S, Benezra M, Rosario L, Tew K, Pincus M, Sardana M, Henderson C, Wolf CR, *et al.* (1999). Regulation of JNK signaling by GSTp. EMBO J 18, 1321–1334.

Adomavicius T, Guaita M, Zhou Y, Jennings MD, Latif Z, Roseman AM, Pavitt GD (2019). The structural basis of translational control by eIF2 phosphorylation. Nat Commun 10, 2136.

Advani VM, Ivanov P (2020). Stress granule subtypes: an emerging link to neurodegeneration. Cell Mol Life Sci 77, 4827–4845.

Aguilera-Gomez A, Zacharogianni M, van Oorschot MM, Genau H, Grond R, Veenendaal T, Sinsimer KS, Gavis EA, Behrends C, Rabouille C (2017). Phospho-Rasputin Stabilization by Sec16 Is Required for Stress Granule Formation upon Amino Acid Starvation. Cell Rep 20, 935–948.

Alam U, Kennedy D (2019). Rasputin a decade on and more promiscuous than ever? A review of G3BPs. Biochim Biophys Acta - Mol Cell Res 1866, 360–370.

Alberti S, Mateju D, Mediani L, Carra S (2017). Granulostasis: Protein quality control of RNP granules. Front Mol Neurosci 10, 84.

Allocati N, Masulli M, Di Ilio C, Federici L (2018). Glutathione transferases: Substrates, inihibitors and pro-drugs in cancer and neurodegenerative diseases. Oncogenesis 7, 8.

Anderson P, Kedersha N (2006). RNA granules. J Cell Biol 172, 803–808.

Anderson P, Kedersha N, Ivanov P (2015). Stress granules, P-bodies and cancer. Biochim Biophys Acta - Gene Regul Mech 1849, 861–870.

Asadi MR, Sadat Moslehian M, Sabaie H, Jalaiei A, Ghafouri-Fard S, Taheri M, Rezazadeh M (2021). Stress Granules and Neurodegenerative Disorders: A Scoping Review. Front Aging Neurosci 13, 650740.
Bakthavachalu B, Huelsmeier J, Sudhakaran IP, Hillebrand J, Singh A, Petrauskas A, Thiagarajan D, Sankaranarayanan M, Mizoue L, Anderson E, *et al*. (2018). RNP-Granule Assembly via Ataxin-2 Disordered Domains Is Required for Long-Term Memory and Neurodegeneration. Neuron. 98, 754–766.
Balchin D, Hayer-Hartl M, Hartl FU (2016). In vivo aspects of protein folding and quality control. Science 353, aac4354.
Bansal P, Madlung J, Schaaf K, Macek B, Bono F (2020). An Interaction Network of RNA-Binding Proteins Involved in *Drosophila* Oogenesis. Mol Cell Proteomics 19, 1485–1502.
Battich N, Beumer J, De Barbanson B, Krenning L, Baron CS, Tanenbaum ME, Clevers H, Van Oudenaarden A (2020). Sequencing metabolically labeled transcripts in single cells reveals mRNA turnover strategies. Science 367, 1151–1156.
Bäuerlein FJB, Saha I, Mishra A, Kalemanov M, Martínez-Sánchez A, Klein R, Dudanova I, Hipp M, Hartl FU, Baumeister W, *et al*. (2017). In Situ Architecture and Cellular Interactions of PolyQ Inclusions. Cell 171, 179–187.
Baumgartner R, Stocker H, Hafen E (2013). The RNA-binding Proteins FMR1, Rasputin and Caprin Act Together with the UBA Protein Lingerer to Restrict Tissue Growth in *Drosophila melanogaster*. PLoS Genet 9, e1003598.
Bijlsma R, Loeschcke V (2005). Environmental stress, adaptation and evolution: An overview. J Evol Biol 18, 744–749.
Blatt P, Wong-Deyrup SW, McCarthy A, Breznak S, Hurton MD, Upadhyay M, Bennink B, Camacho J, Lee MT, Rangan P (2021). RNA degradation sculpts the maternal transcriptome during *Drosophila* oogenesis. Curr Biol 31, 2984–2994.
Blevins WR, Tavella T, Moro SG, Blasco-Moreno B, Closa-Mosquera A, Díez J, Carey LB, Albà MM (2019). Extensive post-transcriptional buffering of gene expression in the response to severe oxidative stress in baker's yeast. Sci Rep 9, 11005.
Bozaykut P, Ozer NK, Karademir B (2014). Regulation of protein turnover by heat shock proteins. Free Radic Biol Med 77, 195–209.
Bratkovič T, Bozič J, Rogelj B (2020). Functional diversity of small nucleolar RNAs. Nucleic Acids Res 48, 1627–1651.
Brown JB, Boley N, Eisman R, May GE, Stoiber MH, Duff MO, Booth BW, Wen J, Park S, Suzuki AM, *et al*. (2014). Diversity and dynamics of the *Drosophila* transcriptome. Nature 512, 393–399.
De Bruijn FJ (2016). Stress and Environmental Regulation of Gene Expression and Adaptation in Bacteria. ISBN: 978-1-119-00488-2.
Buddika K, Ariyapala IS, Hazuga MA, Riffert D, Sokol NS (2020). Canonical nucleators are dispensable for stress granule assembly in intestinal progenitors. J Cell Sci 133, jcs24351.
Chan HYE, Warrick JM, Gray-Board GL, Paulson HL, Bonini NM (2000). Mechanisms of chaperone suppression of polyglutamine disease: Selectivity, synergy and modulation of protein solubility in *Drosophila*. Hum Mol Genet 9, 2811–2820.
Chen D, Dale RK, Lei EP (2018). Shep regulates *Drosophila* neuronal remodeling by controlling transcription of its chromatin targets. Dev 145, dev154047.
Chowdhary S, Kainth AS, Pincus D, Gross DS (2019). Heat Shock Factor 1 Drives Intergenic Association of Its Target Gene Loci upon Heat Shock. Cell Rep 26, 18–28.
Colinet H, Hoffmann A (2010). Gene and protein expression of *Drosophila* Starvin during cold stress and recovery from chill coma. Insect Biochem Mol Biol 40, 425–428.
Colinet H, Lee SF, Hoffmann A (2010). Temporal expression of heat shock genes during cold stress and recovery from chill coma in adult *Drosophila melanogaster*. FEBS J 277, 174–185.
Connerty P, Lock RB, Bock de CE (2020). Long Non-coding RNAs: Major Regulators of Cell Stress in Cancer. Front Oncol 10, 285.
Costa-Mattioli M, Walter P (2020). The integrated stress response: From mechanism to disease. Science 368, eaat5314.
Dahl JU, Gray MJ, Jakob U (2015). Protein quality control under oxidative stress conditions. J Mol Biol 427, 1549–1563.
Donovan M, Marr M (2015). dFoxo Dependent Transcription of the Heat Shock Proteins. Faseb J 29.
Doonan LB, Hartigan A, Okamura B, Long PF (2019). Stress-Free Evolution: The Nrf-Coordinated Oxidative Stress Response in Early Diverging Metazoans. Integr Comp Biol 59, 799–810.
Escalante LE, Gasch AP (2021). The role of stress-activated RNA–protein granules in surviving adversity. RNA 27, 753–762.
Falaleeva M, Pages A, Matuszek Z, Hidmi S, Agranat-Tamir L, Korotkov K, Nevo Y, Eyras E, Sperling R, Stamm S (2016). Dual function of C/D box small nucleolar RNAs in rRNA modification and alternative pre-mRNA splicing. Proc Natl Acad Sci USA 113, E1625–E1634.
Fare CM, Shorter J (2021). (Dis)Solving the problem of aberrant protein states. Dis Model Mech 14, dmm048983.
Farny NG, Kedersha NL, Silver PA (2009). Metazoan stress granule assembly is mediated by P-eIF2α-dependent and -independent mechanisms. RNA 15, 1814–1821.
Fedoroff N (2006). Redox regulatory mechanisms in cellular stress responses. Ann Bot 98, 289–300.
Finka A, Mattoo RUH, Goloubinoff P (2016). Experimental Milestones in the Discovery of Molecular Chaperones as Polypeptide Unfolding Enzymes. Annu Rev Biochem 85, 715–742.
Fung G, Chen S, Zhang J, Shi J, Wong J, Piesik P, Han L, Chu F, Jagdeo J, Jan E, Fujita T, *et al*. (2013). Production of a dominant-negative fragment due to G3BP1 cleavage contributes to the disruption of mitochondria-associated protective stress granules during CVB3 infection. PLoS One 8, e79546.
Ganassi M, Mateju D, Bigi I, Mediani L, Poser I, Lee HO, Seguin SJ, Morelli FF, Vinet J, Leo G, *et al*. (2016). A Surveillance Function of the HSPB8-BAG3-HSP70 Chaperone Complex Ensures Stress Granule Integrity and Dynamism. Mol Cell 63, 796–810.
Gasset-Rosa F, Lu S, Yu H, Chen C, Melamed Z, Guo L, Shorter J, Da Cruz S, Cleveland DW (2019). Cytoplasmic TDP-43 De-mixing Independent of Stress Granules Drives Inhibition of Nuclear Import, Loss of Nuclear TDP-43, and Cell Death. Neuron 102, 339–357.
Geser F, Robinson JL, Malunda JA, Xie SX, Clark CM, Kwong LK, Moberg PJ, Moore EM, Van Deerlin VM, Lee VMY, *et al*. (2010). Pathological 43-kDa transactivation response DNA-binding protein in older adults with and without severe mental illness. Arch Neurol 67, 1238–1250.
Gidalevitz T, Prahlad V, Morimoto RI (2011). The stress of protein misfolding: From single cells to multicellular organisms. Cold Spring Harb Perspect Biol, a009704.
Ginsberg SD, Galvin JE, Chiu TS, Lee VMY, Masliah E, Trojanowski JQ (1998). RNA sequestration to pathological lesions of neurodegenerative diseases. Acta Neuropathol 96, 487–494.
Gitter A, Carmi M, Barkai N, Bar-Joseph Z (2013). Linking the signaling cascades and dynamic regulatory networks controlling stress responses. Genome Res 23, 365–376.
Gong WJ, Golic KG (2006). Loss of Hsp70 in *Drosophila* is pleiotropic, with effects on thermotolerance, recovery from heat shock and neurodegeneration. Genetics 172, 275–286.
Guillén-Boixet J, Kopach A, Holehouse AS, Wittmann S, Jahnel M, Schlüßler R, Kim K, Trussina IREA, Wang J, Mateju D, *et al*. (2020). RNA-Induced Conformational Switching and Clustering of G3BP Drive Stress Granule Assembly by Condensation. Cell 181, 346–361.
Halliday M, Radford H, Zents KAM, Molloy C, Moreno JA, Verity NC, Smith E, Ortori CA, Barrett DA, Bushell M, Mallucci GR (2017). Repurposed drugs targeting eIF2α-P-mediated translational repression prevent neurodegeneration in mice. Brain 140, 1768–1783.
He H, Van Breusegem F, Mhamdi A (2018). Redox-dependent control of nuclear transcription in plants. J Exp Bot 69, 3359–3372.
Hinnebusch AG (2017). Structural Insights into the Mechanism of Scanning and Start Codon Recognition in Eukaryotic Translation Initiation. Trends Biochem Sci 42, 589–611.
Hu Y, Comjean A, Roesel C, Vinayagam A, Flockhart I, Zirin J, Perkins L, Perrimon N, Mohr SE (2017). FlyRNAi.org - The database of the *Drosophila* RNAi screening center and transgenic RNAi project: 2017 update. Nucleic Acids Res 45, D672–D678.
Huelsmeier J, Walker E, Bakthavachalu B, Ramaswami M (2021). A C-terminal ataxin-2 disordered region promotes Huntingtin protein aggregation and neurodegeneration in *Drosophila* models of Huntington's disease. G3 GenesIGenomesIGenetics 11, jkab355.
Huen NYM, Chan HYE (2005). Dynamic regulation of molecular chaperone gene expression in polyglutamine disease. Biochem Biophys Res Commun 334, 1074–1084.
Ivanov P, Kedersha N, Anderson P (2019). Stress granules and processing bodies in translational control. Cold Spring Harb Perspect Biol 11, a032813.
Jacobson T, Navarrete C, Sharma SK, Sideri TC, Ibstedt S, Priya S, Grant CM, Christen P, Goloubinoff P, Tamá MJ (2012). Arsenite interferes with protein folding and triggers formation of protein aggregates in yeast. J Cell Sci 125, 5073–5083.
Jain S, Wheeler JR, Walters RW, Agrawal A, Barsic A, Parker R (2016). ATPase-Modulated Stress Granules Contain a Diverse Proteome and Substructure. Cell 164, 487–498.

Jao CY, Salic A (2008). Exploring RNA transcription and turnover in vivo by using click chemistry. Proc Natl Acad Sci USA 105, 15779–15784.
Kedersha N, Panas MD, Achorn CA, Lyons S, Tisdale S, Hickman T, Thomas M, Lieberman J, McInerney GM, Ivanov P, *et al.* (2016). G3BP-Caprin1-USP10 complexes mediate stress granule condensation and associate with 40S subunits. J Cell Biol 212, 845–860.
Kedersha N, Anderson P (2002). Stress granules: Sites of mRNA triage that regulate mRNA stability and translatability. Biochem Soc Trans 30, 963–969.
Kedersha N, Anderson P (2007). Mammalian Stress Granules and Processing Bodies. Methods Enzymol 431, 61–81.
Kedersha N, Gupta M, Li W, Miller I, Anderson P (1999). RNA-binding proteins TIA-1 and TIAR link the phosphorylation of eIF-2α to the assembly of mammalian stress granules. J Cell Biol. 147, 1431–1441.
Khong A, Matheny T, Jain S, Mitchell SF, Wheeler JR, Parker R (2017). The Stress Granule Transcriptome Reveals Principles of mRNA Accumulation in Stress Granules. Mol Cell 68, 808–820.
Kishore S, Khanna A, Zhang Z, Hui J, Balwierz PJ, Stefan M, Beach C, Nicholls RD, Zavolan M, Stamm S (2010). The snoRNA MBII-52 (SNORD 115) is processed into smaller RNAs and regulates alternative splicing. Hum Mol Genet 19, 1153–1164.
Kishore S, Stamm S (2006). The snoRNA HBII-52 regulates alternative splicing of the serotonin receptor 2C. Science 311, 230–232.
Krukowski K, Nolan A, Frias ES, Boone M, Ureta G, Grue K, Paladini MS, Elizarraras E, Delgado L, Bernales S, *et al.* (2020). Small molecule cognitive enhancer reverses age-related memory decline in mice. Elife 9, e62048.
Kufel J, Grzechnik P (2019). Small Nucleolar RNAs Tell a Different Tale. Trends Genet 35, 104–117.
Kültz D (2003). Evolution of the cellular stress proteome: From monophyletic origin to ubiquitous function. J Exp Biol 206, 3119–3124.
Laborde E (2010). Glutathione transferases as mediators of signaling pathways involved in cell proliferation and cell death. Cell Death Differ 17, 1728–1737.
Lakhotia SC (2012). Long non-coding RNAs coordinate cellular responses to stress. Wiley Interdiscip Rev RNA 3, 779–796.
Laver JD, Ly J, Winn AK, Karaiskakis A, Lin S, Nie K, Benic G, Jaberi-Lashkari N, Cao WXi, Khademi A, *et al.* (2020). The RNA-Binding Protein Rasputin/G3BP Enhances the Stability and Translation of Its Target mRNAs. Cell Rep 30, 3353–3367.
Lee AK, Klein J, Fon Tacer K, Lord T, Oatley MJ, Oatley JM, Porter SN, Pruett-Miller SM, Tikhonova EB, Karamyshev AL, *et al.* (2020). Translational Repression of G3BP in Cancer and Germ Cells Suppresses Stress Granules and Enhances Stress Tolerance. Mol Cell 79, 645–659.
Lee J, Harris AN, Holley CL, Mahadevan J, Pyles KD, Lavagnino Z, Scherrer DE, Fujiwara H, Sidhu R, Zhang J, *et al.* (2016). Rpl13a small nucleolar RNAs regulate systemic glucose metabolism. J Clin Invest 126, 4616–4625.
Lee Y, Rio DC (2015). Mechanisms and regulation of alternative Pre-mRNA splicing. Annu Rev Biochem 84, 291–323.
Van Leeuwen W, Vaninsberghe M, Battich N, Salmén F, Van Oudenaarden A, Rabouille C (2021). Identification of the stress granule transcriptome via RNA-editing in single cells and in vivo. BioRxiv 06.21, 449212.
Liu Z, Zhang S, Gu J, Tong Y, Li Y, Gui X, Long H, Wang C, Zhao C, Lu J, *et al.* (2020). Hsp27 chaperones FUS phase separation under the modulation of stress-induced phosphorylation. Nat Struct Mol Biol 27, 363–372.
Ly LD, Xu S, Choi SK, Ha CM, Thoudam T, Cha SK, Wiederkehr A, Wollheim CB, Lee IK, Park KS (2017). Oxidative stress and calcium dysregulation by palmitate in type 2 diabetes. Exp Mol Med 49, e291.
Mailloux RJ, McBride SL, Harper ME (2013). Unearthing the secrets of mitochondrial ROS and glutathione in bioenergetics. Trends Biochem Sci 38, 592–602.
Mateju D, Franzmann TM, Patel A, Kopach A, Boczek EE, Maharana S, Lee HO, Carra S, Hyman AA, Alberti S (2017). An aberrant phase transition of stress granules triggered by misfolded protein and prevented by chaperone function. EMBO J 36, 1669–1687.
McCormick C, Khaperskyy DA (2017). Translation inhibition and stress granules in the antiviral immune response. Nat Rev Immunol 17, 647–660.
Michaud S, Marin R, Tanguay RM (1997). Regulation of heat shock gene induction and expression during *Drosophila* development. Cell Mol Life Sci 53, 104–113.
Michel CI, Holley CL, Scruggs BS, Sidhu R, Brookheart RT, Listenberger LL, Behlke MA, Ory DS, Schaffer JE (2011). Small nucleolar RNAs U32a, U33, and U35a are critical mediators of metabolic stress. Cell Metab 14, 33–44.
Milton VJ, Sweeney ST (2012). Oxidative stress in synapse development and function. Dev Neurobiol 72, 100–110.
Mittal D, Madhyastha DA, Grover A (2012). Genome-wide transcriptional profiles during temperature and oxidative stress reveal coordinated expression patterns and overlapping regulons in rice. PLoS One 7, e40899.
Mogk A, Ruger-Herreros C, Bukau B (2019). Cellular Functions and Mechanisms of Action of Small Heat Shock Proteins. Annu Rev Microbiol 73, 89–110.
Morano KA, Grant CM, Moye-Rowley WS (2012). The response to heat shock and oxidative stress in *Saccharomyces cerevisiae*. Genetics 190, 1157–1195.
Morimoto RI (1998). Regulation of the heat shock transcriptional response: Cross talk between a family of heat shock factors, molecular chaperones, and negative regulators. Genes Dev 12, 3788–3796.
Pazman C, Mayes CA, Fanto M, Haynes SR, Mlodzik M (2000). Rasputin, the *Drosophila* homologue of the RasGAP SH3 binding protein, functions in Ras- and Rho-mediated signaling. Development 127, 1715–1725.
Perez LB, Brown PJ (2014). The role of ROS signaling in cross-tolerance: From model to crop. Front Plant Sci 5, 754.
Rabani M, Levin JZ, Fan L, Adiconis X, Raychowdhury R, Garber M, Gnirke A, Nusbaum C, Hacohen N, Friedman N, *et al.* (2011). Metabolic labeling of RNA uncovers principles of RNA production and degradation dynamics in mammalian cells. Nat Biotechnol 29, 436–442.
Radford H, Moreno JA, Verity N, Halliday M, Mallucci GR (2015). PERK inhibition prevents tau-mediated neurodegeneration in a mouse model of frontotemporal dementia. Acta Neuropathol 130, 633–642.
Rebeaud ME, Mallik S, Goloubinoff P, Tawfik DS (2021). On the evolution of chaperones and co-chaperones and the exponential expansion of proteome complexity. Proc Natl Acad Sci 118, e2020885118.
Reichmann D, Voth W, Jakob U (2018). Maintaining a Healthy Proteome during Oxidative Stress. Mol Cell 69, 203–213.
Ron D (2002). Translational control in the endoplasmic reticulum stress response. J Clin Invest 110, 1383–1388.
Ruiz-Ramos R, Lopez-Carrillo L, Rios-Perez AD, De Vizcaya-Ruíz A, Cebrian ME (2009). Sodium arsenite induces ROS generation, DNA oxidative damage, HO-1 and c-Myc proteins, NF-κB activation and cell proliferation in human breast cancer MCF-7 cells. Mutat Res - Genet Toxicol Environ Mutagen 674, 109–115.
Sanders DW, Kedersha N, Lee DSW, Strom AR, Drake V, Riback JA, Bracha D, Eeftens JM, Iwanicki A, Wang A, *et al.* (2020). Competing Protein-RNA Interaction Networks Control Multiphase Intracellular Organization. Cell 181, 306–324.
Schieber M, Chandel NS (2014). ROS function in redox signaling and oxidative stress. Curr Biol 24, R453–R462.
Somasekharan SP, Zhang F, Saxena N, Huang JN, Kuo IC, Low C, Bell R, Adomat H, Stoynov N, Foster L, *et al.* (2020). G3BP1-linked mRNA partitioning supports selective protein synthesis in response to oxidative stress. Nucleic Acids Res 48, 6855–6873.
Sørensen JG, Nielsen MM, Kruhøffer M, Justesen J, Loeschcke V (2005). Full genome gene expression analysis of the heat stress response in *Drosophila melanogaster*. Cell Stress Chaperones 10, 312–328.
Štětina T, Koštál V, Korbelová J (2015). The role of inducible Hsp70, and other heat shock proteins, in adaptive complex of cold tolerance of the fruit fly (*Drosophila melanogaster*). PLoS One 10, e0128976.
Sudhakaran IP, Hillebrand J, Dervan A, Das S, Holohan EE, Hülsmeier J, Sarov M, Parker R, VijayRaghavan K, Ramaswami M (2014). FMRP and Ataxin-2 function together in long-term olfactory habituation and neuronal translational control. Proc Natl Acad Sci USA 111, E99–E108.
Szabo EX, Reichert P, Lehniger MK, Ohmer M, de Francisco Amorim M, Gowik U, Schmitz-Linneweber C, Laubinger S (2020). Metabolic Labeling of RNAs Uncovers Hidden Features and Dynamics of the *Arabidopsis* Transcriptome. Plant Cell 32, 871–887.
Tian G, Hu C, Yun Y, Yang W, Dubiel W, Cheng Y, Wolf DA (2021). Dual roles of HSP70 chaperone HSPA1 in quality control of nascent and newly synthesized proteins. EMBO J 40, e106183.
Torrent M, Chalancon G, De Groot NS, Wuster A, Madan Babu M (2018). Cells alter their tRNA abundance to selectively regulate protein synthesis during stress conditions. Sci Signal 11, eaat6409.
Tsai W-C, Lloyd RE (2014). Cytoplasmic RNA Granules and Viral Infection. Annu Rev Virol 1, 147–170.
Veal EA, Mark Toone W, Jones N, Morgan BA (2002). Distinct roles for glutathione S-transferases in the oxidative stress response in *Schizosaccharomyces pombe*. J Biol Chem 277, 35523–35531.

Vendredy L, Adriaenssens E, Timmerman V (2020). Small heat shock proteins in neurodegenerative diseases. Cell Stress Chaperones 25, 679–699.

Verghese J, Abrams J, Wang Y, Morano KA (2012). Biology of the Heat Shock Response and Protein Chaperones: Budding Yeast (*Saccharomyces cerevisiae*) as a Model System. Microbiol Mol Biol Rev 76, 115–158.

Vert G, Chory J (2011). Crosstalk in Cellular Signaling: Background Noise or the Real Thing? Dev Cell 21, 985–991.

Vihervaara A, Duarte FM, Lis JT (2018). Molecular mechanisms driving transcriptional stress responses. Nat Rev Genet 19, 385–397.

Vihervaara A, Mahat DB, Guertin MJ, Chu T, Danko CG, Lis JT, Sistonen L (2017). Transcriptional response to stress is pre-wired by promoter and enhancer architecture. Nat Commun 8, 255.

Vos MJ, Carra S, Kanon B, Bosveld F, Klauke K, Sibon OCM, Kampinga HH (2016). Specific protein homeostatic functions of small heat-shock proteins increase lifespan. Aging Cell 15, 217–226.

Walters RW, Muhlrad D, Garcia J, Parker R (2015). Differential effects of Ydj1 and Sis1 on Hsp70-mediated clearance of stress granules in *Saccharomyces cerevisiae*. RNA 21, 1660–1671.

Wang AM, Miyata Y, Klinedinst S, Peng HM, Chua JP, Komiyama T, Li X, Morishima Y, Merry DE, Pratt WB, *et al*. (2013). Activation of Hsp70 reduces neurotoxicity by promoting polyglutamine protein degradation. Nat Chem Biol 9, 112–118.

Warrick JM, Chan HYE, Gray-Board GL, Chai Y, Paulson HL, Bonini NM (1999). Suppression of polyglutamine-mediated neurodegeneration in *Drosophila* by the molecular chaperone HSP70. Nat Genet 23, 425–428.

Webster JM, Darling AL, Uversky VN, Blair LJ (2019). Small heat shock proteins, big impact on protein aggregation in neurodegenerative disease. Front Pharmacol 10, 1047.

Wheeler JR, Matheny T, Jain S, Abrisch R, Parker R (2016). Distinct stages in stress granule assembly and disassembly. Elife 5, e18413.

Wohlbach DJ, Thompson DA, Gasch AP, Regev A (2009). From elements to modules: regulatory evolution in Ascomycota fungi. Curr Opin Genet Dev 19, 571–578.

Wolozin B, Ivanov P (2019). Stress granules and neurodegeneration. Nat Rev Neurosci 20, 649–666.

Yang P, Mathieu C, Kolaitis RM, Zhang P, Messing J, Yurtsever U, Yang Z, Wu J, Li Y, Pan Q, *et al*. (2020). G3BP1 Is a Tunable Switch that Triggers Phase Separation to Assemble Stress Granules. Cell 181, 325–345.

Yang X, Shen Y, Garre E, Hao X, Krumlinde D, Cvijovi M, Arens C, Nyström T, Liu B, Sunnerhagen P (2014). Stress Granule-Defective Mutants Deregulate Stress Responsive Transcripts. PLoS Genet 10, e1004763.

Yu H, Lu S, Gasior K, Singh D, Vazquez-Sanchez S, Tapia O, Toprani D, Beccari MS, Yates JR, Da Cruz S, *et al*. (2021). HSP70 chaperones RNA-free TDP-43 into anisotropic intranuclear liquid spherical shells. Science 371, eabb4309.

Zhao H, Chen J, Liu J, Han B (2015). Transcriptome analysis reveals the oxidative stress response in Saccharomyces cerevisiae. RSC Adv 5, 22923–22934.

Zou S, Meadows S, Sharp L, Jan LY, Jan YN (2000). Genome-wide study of aging and oxidative stress response in Drosophila melanogaster. Proc Natl Acad Sci USA 97, 13726–13731.